This is to certify that the

thesis entitled

Feasibility Study of a Biosensor
for Biological Processes

presented by

Cynthia Ann Znati

has been accepted towards fulfillment
of the requirements for

M.S. degree in CHE

Dana Bruckis

Major professor

Date 11/11/91

FEASIBILITY STUDY OF A BIOSENSOR FOR BIOLOGICAL PROCESSES

By

Cynthia Ann Znati

A THESIS

Submitted to
Michigan State University
in partial fulfillment of the requirements
for the degree of

MASTER OF SCIENCE

Department of Chemical Engineering

1991

ABSTRACT

FEASIBILITY STUDY OF A BIOSENSOR FOR BIOLOGICAL PROCESSES

By

Cynthia Ann Znati

A biosensor prototype which is potentially fast, reliable, and specific in its response was developed. Glutamate oxidase was chosen as the enzyme for this biosensor because it has many desirable biochemical and kinetic characteristics. A hollow fiber enzymatic reactor (HFER) was used to construct the biosensor. Polysulfone fibers with a molecular weight cutoff of 10,000 were chosen because they had the highest retention of glutamate oxidase.

The hollow fiber sensor was evaluated for its pressure drop characteristics. The resistances and permeabilities of the fiber and of the enzyme were calculated. The resistance of fibers with enzyme increased as the amount of enzyme increased. The pressure drop over the fibers was limited to 10 psi which gave a maximum flow rate $0.3 ml/min$.

The effects of substrate concentration and enzyme loading on the biosensor were measured. Glutamate oxidase was characterized in free solution. The K_m was $0.24\ mM$, and the k was $0.14\ mM\ unit^{-1}\ min^{-1}$ which compare well with the values found in literature. When the biosensor was tested for its response to step changes in glutamate concentration, however, the biosensor did not respond. Since immobilization can affect the activity of enzymes, the kinetic constants were determined *in situ* and for recovered enzyme. The recovered enzyme had an acceptable activity, but the immobilized enzyme was severely affected by the immobilization. This led to a very slow reaction rate and the poor response. Further testing of the immobilized enzyme is required. The "dead" time in the biosensor system is also a cause for the poor response. With some modifications, this biosensor has the potential of becoming a reliable, highly specific on-line biosensor for glutamate. Furthermore, the biosensor can easily be adapted to measure other biological products simply by using another enzyme.

To Mom, Dad, Taieb, and Sami

ACKNOWLEDGEMENTS

I would first like to thank my advisor, Daina M. Briedis for her support, patience, and encouragement. She always helped me find ways around the many difficulties and never gave up on me for these past two years. She also served as a role model to show me that women really can succeed in chemical engineering and have a fulfilling family life also.

Many thanks must go to Steve Reiken who showed me many of the techniques that I used for this research (even though some of them didn't work for me) and helped me to figure out what was not working. Thanks also to Susan Jones, Bharath Rangarajan, Len Czupski, Keith Glassford, and Reena Chakaraborty for the interesting coffee breaks and discussions. I would also like to extend my thanks to the Case Center, and especially to Mike McPherson and Margaret Wilke for their help and technical support.

I am grateful to my entire family. Special thanks go to my parents and sister who never stopped believing in me and encouraging me to do my best. Their support has been invaluable in helping me accomplish this thesis. I wish also to thank my grandmothers and late grandfathers for their moral support.

Most of all, I would like to thank my husband, Taieb, for his help with this thesis. He spent hours, even days, for helping me with the programs, figures and formatting of this thesis. His critical proofreading has certainly improved this work. Without his love, patience and encouragement, this thesis would probably still be a collection of unorganized thoughts.

Last, but definitely not least, I must thank my son Sami Amin whose appearance may perhaps have delayed this thesis, but certainly brought much joy to my heart. When life seemed too much to handle, his smile and his playful antics kept me going.

TABLE OF CONTENTS

List of Tables

List of Figures

Chapter 1

Introduction

In recent years, the use of biological products and processes in the chemical and medical fields has been rapidly gaining importance. The increasing interest in the economic production and quality control of biological products raises the need for effective control of bioreactors. The research reported in this thesis focuses mainly on the development of fast, reliable detection methods for biological processes. The goal of this research has been to develop a biosensor that is potentially fast, reliable, and specific in its response for the measurement of amino acid concentrations.

In the remainder of this chapter, the specific research problem will be explained in detail and the reason for developing an on-line biosensor will be presented. I then discuss the choice of the enzyme/substrate system and conclude the chapter by setting forth the organization of this thesis.

1.1 Problem Description

Biological processes have been used for centuries in the production of foodstuffs (wine, beer, cheese, yogurt, vinegar, etc.); however, in recent years, biological processes have become important in other fields. Not only are biological processes used in the manufacture of pharmaceuticals, but biochemical and biological products are used

extensively for assays. Waste treatment is another field that uses biological processes. Traditionally, waste water has been decontaminated by bacteria. Composting depends on microorganisms to decompose the biodegradable material. Recently, microorganisms have been developed that degrade toxic wastes and oil. The use of biological fermentations in the food and beverage industries is still prevalent.

As the use of biological products has increased, so has the need for effective control of bioreactors. Biological catalysts, whether they are enzymes or whole cells, are very sensitive to environmental conditions. Relatively small changes in pH and temperature or low concentrations of inhibitors or biocidal agents can drastically affect the performance of a bioreactor. Temperature and pH can be quickly measured and easily controlled. On the other hand, detection of biological inhibitors or biocidal agents can be quite difficult. Because inhibitors often closely resemble substrates, the analytical detection methods must be very precise. These methods often require complicated steps and lengthy incubation times. It could take several hours before the presence of an inhibitor or biocidal agent is detected. In that time, the inhibitor or biocidal agent could reduce the output of the bioreactor significantly.

Other types of macromolecules also need to be detected. The performance of continuous reactors is often measured by analyzing the outputs of the reactors. Batch reactors are often monitored to follow the course of the reaction to determine when to terminate the reaction. As with the detection of inhibitors and biocidal agents, analysis can take several hours. For continuous reactors, this would mean that several hours' worth of output may not meet specifications if the reactor's performance is poor. For batch reactors, the reaction may proceed too far and produce unwanted by-products.

For these reasons, it is important to develop fast, reliable detection methods for biological processes. Most current assays for biological compounds require that a sample be removed from the reaction vessel and taken to a laboratory for analysis. Detection

methods should ideally be on-line and should give results within a few minutes. These methods should also be very specific and should not have many interfering substrates.

The biosensor that was developed for this thesis will meet most of these requirements. It was designed for on-line analysis. The response of the biosensor has the potential to be very fast, and the biosensor itself can be very specific depending on the enzyme that is used.

Glutamate oxidase was chosen as the enzyme for this biosensor because it has many desirable characteristics. The enzyme is stable as a freeze-dried powder and, hence, is very easy to transport and store. Glutamate oxidase is very specific for glutamate and has virtually no other substrate. In addition, it has a low K_m for glutamate which indicates a high affinity for glutamate. The enzyme is relatively thermostable and has a good tolerance for pH [1].

Glutamate itself is an important compound for analysis. It is a major flavor enhancer and is found in monosodium glutamate (MSG) and soy sauce. The fermentation time of soy sauce is actually determined by the glutamate concentration [2,3]. Glutamate is also involved in the metabolic pathways of all amino acids. All α-amino groups are derived directly or indirectly from ammonia through the amino group of L-glutamate. This relationship is shown in Figure 1.1. The deaminated form of glutamate, α-ketoglutarate, is the gateway into the Krebs cycle. Hence, the use of amino acids for energy in cells requires the presence of glutamate [4].

Based on these reasons, the system chosen for study in this biosensor was the glutamate/glutamate oxidase system; however, any analyte could be used in this biosensor as long as an appropriate enzyme could be found.

This biosensor was constructed as a hollow fiber enzymatic reactor (HFER). The enzyme was immobilized in the macroporous region of a hollow fiber. This region served as the reaction portion of the sensor. The lumen of the fiber carried the effluent to

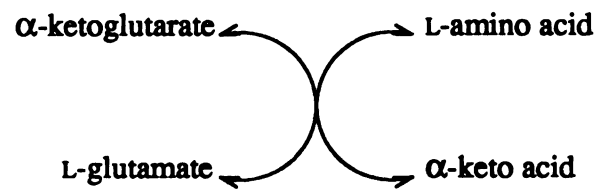

Figure 1.1. Interaction of Glutamate and Amino Acids in the Krebs Cycle

detection.

1.2 Organization of Thesis

In this chapter the reasons for development of an on-line biosensor were presented. The choice of enzyme/substrate system and the overall design of the biosensor were briefly discussed. Chapter 2 contains background information pertinent to the development of this biosensor. Previous designs of biosensors are discussed, and their relative advantages and disadvantages are noted. Mathematical models are presented for the HFER, and their solutions are discussed. In Chapter 3, the materials and methods used in developing the biosensor are described. In addition, the procedure that was used to evaluate and assess the suitability of the compounds of the enzymic reaction for on-line detection is presented. Chapter 4 presents the results of the experiments and discusses their significance. Modifications to the design of the biosensor are also suggested. Chapter 5 summarizes the main contributions of this research project and describes further extension of this work.

Chapter 2

Literature Review

The increasing use of biological processes has created a need for fast, sensitive detection of biological compounds. These detection methods are used in both clinical and industrial settings. In the industrial setting, detection of biological compounds is very important for the control of bioreactors. Bioreactors are very sensitive and need to be monitored closely. A small change in the concentration of a product or inhibitor can dramatically alter the contents of a fermenter. In addition, product yields can be enhanced by maintaining the concentrations of reactants or products at a certain level. To do this successfully, concentrations must be quickly and accurately determined. Due to small sample size and generally low concentrations in body fluids, detection in clinical settings has its own set of difficulties. This thesis will only focus on detection in industrial settings.

The purpose of this chapter is to describe the current biosensor technologies and discuss their advantages and limitations. The models that have been employed to describe hollow fiber reactors will also be discussed.

2.1 Current Biosensor Technology

In the following sections, the current biosensor technology is reviewed. The design of these biosensors is described, and their advantages and disadvantages are discussed.

2.1.1 Enzyme Electrodes

One of the most common types of biosensors is the enzyme electrode. The electrode is specific for a product or reactant of an enzymic reaction. The enzyme electrode has two major advantages. First, enzymes are generally very specific for their substrates which allows detection to be very specific also. Second, electrodes can be easily adapted for on-line measurements. The disadvantages, which vary according to the specific enzyme electrode that is used, include short lifetimes, signal drift, weak signals, and long response times. Little can be done to alleviate these problems because they are inherent to the electrode.

Guilbault and Shu developed urea and L-tyrosine electrodes [5]. The enzyme electrodes were identical except for the enzyme used. Both reactions were decarboxylations and are shown below:

$$urea \xrightarrow{urease} 2NH_3 + CO_2 \qquad (2.1)$$

$$tyrosine \xrightarrow[decarboxylase]{tyrosine} tyramine + CO_2 \qquad (2.2)$$

The enzymes were placed on the tip of a carbon dioxide electrode and held in place by dialysis paper. Since no chemical means of immobilization were used, the enzymes retained their free solution kinetics. However, diffusion played a very important role in the reaction. When the enzyme electrodes were placed in their respective sample solutions, voltage readings were produced. The analyte (urea or tyrosine) diffused through the dialysis paper and reacted to form the carbon dioxide and other products. The carbon dioxide diffused through the gas permeable membrane of the carbon dioxide electrode into the internal filling solution. The filling solution was $NaHCO_3$, and the change in pH

caused by the carbon dioxide was measured by a pH electrode. There were several disadvantages for this enzyme electrode: the signal tended to drift at high concentrations, the response time increased for low concentrations, and the response time increased with extended use of the electrode. The lower limit of detection was 0.1 mM CO_2, and the response time was as long as five minutes. At high carbon dioxide concentrations, loss of carbon dioxide to the surroundings could cause the signal drift. The other disadvantages were due mainly to mass transfer resistance. Long response times for low concentrations could indicate increased diffusion times, and increasing response times could indicate decreased enzyme activity.

White and Guilbault used a carbon dioxide enzyme electrode to determine the concentration of another amino acid [6]. In this case, the amino acid was L-lysine and the enzyme was L-lysine decarboxylase. The reaction is similar to those in Equations (2.1) and (2.2). The theory of the analysis and preparation was the same as for the previous electrodes. There were two major differences between this electrode and the previous one. First, the enzyme was co-immobilized with bovine serum albumin to increase stability. Second, the enzyme and protein were cross-linked with glutaraldehyde onto the gas permeable membrane of an electrode, so the dialysis paper was unnecessary. One caveat with this method was that the immobilized enzyme layer eventually pulled loose from the electrode. One advantage with this immobilization technique was that the enzyme showed an increase in activity. The major disadvantages with this electrode were its long response and recovery times. The total time required for an assay was up to 30 minutes. While this was an improvement over previous techniques, it was still too long for on-line control.

Belghith, Romette, and Thomas used a similar technique with an oxygen electrode [7]. The enzyme used was alcohol oxidase which catalyzes the following reactions:

$$CH_3OH + O_2 \longrightarrow H_2O_2 + HCOOH \quad (2.3)$$

$$CH_3CH_2OH + O_2 \longrightarrow H_2O_2 + CH_3COOH \quad (2.4)$$

The enzyme was again immobilized on the gas permeable membrane of the electrode. However, in this case, the gas permeable membrane was first removed and placed on a glass plate. The enzyme was dissolved in a 5% gelatin solution and spread on the membrane. The gelatin-membrane bilayer was dried and then immersed in a 1.25% glutaraldehyde solution to immobilize the enzyme. The electrode was reassembled with this membrane. Because the enzyme was more firmly attached to the gas permeable membrane, this procedure prevented the loosening of the immobilized enzyme layer which had caused difficulties with the L-lysine decarboxylase electrode developed by White and Guilbault [6].

This alcohol electrode had a response time of less than 10 seconds. However, the electrode needed to be replenished with oxygen after each measurement to ensure a good response for the next measurement, so the electrode was rinsed with a buffer and then air. This increased the total measuring time to two minutes for each sample, which is a fast total detection time.

The main disadvantage of this method was that the signal of the electrode decreased with use. In addition, a high concentration of alcohol caused a faster decrease in the signal than a low concentration. For concentrations less than 0.1 M, the electrode could measure up to 600 samples before a significant decline in the signal, but for concentrations greater than 0.5 M, the electrode signal started to decrease as soon as after 200 measurements. This electrode may require frequent replacement which may be a serious

disadvantage.

An enzyme electrode for glutamine that is very similar to the alcohol electrode was developed by Romette and Cooney [8]. This sensor immobilized the two enzymes, glutaminase and glutamate oxidase, on the electrode. The enzymes worked in series and catalyzed the following reactions:

$$glutamine + H_2O \xrightarrow{glutaminase} \text{L-}glutamate + NH_3 \qquad (2.5)$$

$$\text{L-}glutamate + O_2 + H_2O \xrightarrow[oxidase]{glutamate} \alpha\text{–}ketoglutarate + H_2O_2 + NH_3 \qquad (2.6)$$

This sensor also used an oxygen electrode as the basis of measurement. The immobilization technique was exactly the same as for the alcohol electrode. As with the alcohol electrode, the response time was very fast, but again, the electrode needed regeneration with oxygen which brought the total measurement time to two minutes.

The only disadvantage of this sensor was that the activity of the enzymes decreased rapidly with time. When the sensor was stored, it had only 65% of its original activity after 30 days. When the enzyme was used, it retained 90% of its original activity after 300 measurements for low concentrations (0.5 M), but the activity decreased significantly to 40% of its original activity for high concentrations (1.5 M).

Yamauchi *et al.* also used an enzyme electrode to detect glutamate [9]. The enzyme used was again L-glutamate oxidase which catalyzed the reaction in Equation (2.6). The immobilization technique was similar to that used for the oxygen electrodes, but a hydrogen peroxide electrode was used instead of the oxygen electrode. A steady signal was reached in 20 seconds but the signal was very weak. The most probable cause for the

weak signal was mass transfer resistance. The sensor remained stable in storage for 100 days, but was not tested continuously, so its suitability for on-line control is not known.

Many attempts have been made at developing enzyme electrodes. While some have high mass transfer resistances leading to long response times, others have very fast response times. However, all enzyme electrodes have short lifetimes. For fermentations which require long reaction times, the short lifetime of the sensors would necessitate changing the sensors often. This could cause difficulties with the calibration of control equipment.

2.1.2 Biophotodiode

A biophotodiode to measure hydrogen peroxide concentrations was developed by Aizawa *et al.* [10]. This biosensor used the enzyme peroxidase to catalyze the following luminescent reaction:

$$luminol + H_2O_2 \xrightarrow{peroxidase} aminophthalate + N_2 + H_2O + h\nu \qquad (2.7)$$

The luminescence was measure by a silicon photodiode. The reaction was also coupled to the oxidation of glucose by glucose oxidase:

$$\beta\text{-D-}glucose + H_2 + O_2 \xrightarrow[oxidase]{glucose} gluconic\ acid + H_2O_2 \qquad (2.8)$$

The enzymes were immobilized in gel, attached to the photodiode, and covered with a cellulose acetate membrane. The sensor was placed in a sample solution containing luminol and hydrogen peroxide for the single enzyme system or luminol and glucose for the bienzyme system. When photons were released (Eqn. 2.7), the silicon photodiode

produced current proportion to the hydrogen peroxide concentration; however, the current was very weak, 10^{-10} to 10^{-12} A, which indicates high mass transfer resistances. Although the response time of the photodiode is less than 0.5 microseconds, the response time of the whole sensor is over two minutes. The response of the sensor could be limited by the reaction or, more likely, diffusion resistance since the substrate must diffuse through the cellulose acetate membrane and the gel to reach the enzyme. No long term stability studies were carried out, but the authors did note an increase in the standard deviation of the sensor with use. This could indicate inactivation of the enzymes or fouling of the membrane.

2.1.3 Microprobes

Kim and Lee recently developed a microprobe for glucose which is very similar to the enzyme electrode [11]. A platinum wire was coated with glass leaving the tip exposed. The enzyme glucose oxidase was immobilized with glutaraldehyde on the tip and was protected by dipping in a 10% polystyrene acrylonitril solution. The probe detected the hydrogen peroxide produced by the reaction shown in Eqn. 2.8. A Ag/AgCl reference electrode was used as a counter electrode.

The signal produced by the microprobe, although very weak, varied linearly with respect to glucose concentration. The weakness of the signal was not unexpected because the active area on the probe was very small (= 10 $microns^2$). The current was of the same order of magnitude as for the biophotodiode described above. The response time of the sensor was approximately one second, but the response decreased for the first 20 hours of use before it became steady. In addition, because the counter electrode was separate, the response was dependent upon pH. These effects would make calibration difficult. Furthermore, the biosensor was developed to measure local concentrations in microbial film pellets and immobilized cell layers. Therefore, it is too delicate for industrial use.

2.1.4 Amperometric Glucose Sensor

Murakami *et al.* designed a glucose sensor which consisted of a gold micro-electrode with glucose oxidase immobilized in a membrane on the surface [12]. The Ion Selective Field Effect Transistor (ISFET) micro-electrode was prepared with standard integrated circuit (IC) techniques. Glucose oxidase was immobilized over the working electrode using a modified IC technique. The electrode measured the hydrogen peroxide concentration produced by the glucose oxidase reaction, as given by Equation (2.8). Due to the nature of the IC process, this sensor is easily fabricated in large batches.

The electrode had fast, linear response times of approximately 10 seconds for most concentrations. However, the response of the sensor was pH dependent and became non-linear at high concentrations. One caveat that the authors noted was that output drift was substantial. These characteristics of the sensor would make it difficult to calibrate.

Diffusion appeared to have an effect on the sensor although the authors did not discuss this. The signal for the glucose sensor was three orders of magnitude lower than the same sensor used as a hydrogen peroxide sensor. This was most likely caused by diffusional resistance to the substrate in the immobilized enzyme membrane. The main disadvantage to this biosensor is the unprotected state of the enzyme since this sensor was developed for clinical use and is too fragile for the industrial environment.

2.1.5 Continuous Assays with Artificial Membranes

Kolisis and Thomas have developed a sensor which continuously assays for activity of the enzyme neuraminidase [13]. The important reactions are:

$$\textit{sialyllactose} \xrightarrow{\textit{neuraminidase}} \textit{sialic acid} + \textit{lactose} \qquad (2.9)$$

$$\textit{sialic acid} \xrightarrow{\textit{NANA-lyase}} \textit{pyruvate} + \textit{N-acetyl-D-mannosamine} \qquad (2.10)$$

$$\textit{pyruvate} + \textit{NADH} \xrightarrow[\textit{dehydrogenase}]{\textit{lactate}} \textit{lactic acid} + \textit{NAD} \qquad (2.11)$$

The enzymes NANA-lyase and lactate dehydrogenase were immobilized in a gelatin membrane with bovine serum albumin and pyruvate. The membrane was crosslinked with glutaraldehyde which produced a film 70-100 microns thick. The membrane was then placed in a continuous stirred tank reactor (CSTR) which contained sialyllactose, NADH, and neuraminidase. The solution flowed continuously through a spectrophotometer to measure the decrease in NADH concentration. By following the change in NADH concentration, the activity of neuraminidase could be determined. This assay technique could be easily modified to measure concentrations for control of a fermenter.

2.2 Review of Immobilized Enzymes

Enzymes are widely used to catalyze the production of many compounds that would be difficult, even impossible, to synthesize by conventional chemical methods. Enzymes usually have high specificities for their substrates, thus reducing by-products and increasing yields. However, enzymes are also very sensitive to reaction conditions. Temperature, pH, ionic strength, mechanical forces, and organics can affect the performance of enzymes. Therefore, reaction conditions must be closely monitored to prevent denaturation of the enzyme.

Enzymes are obtained from plant, animal, or microbial sources. Since most enzymes are intracellular, extracting and purifying the desired enzyme can be extremely expensive. If the enzyme is used in free solution with the substrate, recovering and

reusing the enzyme from the fermentation broth may be economically necessary. However, this recovery process may be expensive. Therefore, if the enzyme were immobilized on a solid support, it could easily be separated from the fermentation broth. This would facilitate the re-use of the enzyme. In addition, immobilization of the enzyme may increase the stability of the enzyme, thereby increasing the useful lifetime of the enzyme. On the other hand, immobilization may decrease the activity of the enzyme. The effect of immobilization depends on the enzyme and the immobilization procedure itself.

Immobilization techniques may be divided into two classes: chemical methods and physical methods. In chemical methods the enzyme is covalently bonded to a support, whereas the enzyme is physically entrapped by the support when physical methods are used. Chemical methods of immobilization include bonding the enzyme to an insoluble matrix support and cross-linking the enzyme to itself, to other enzymes, or to a support. Physical methods include adsorption to a support, entrapment within a microcapsule or gel matrix, and entrapment in spun or hollow fibers. In general, chemical immobilization is difficult and expensive, but the enzymes retain a high activity and may be more stable. On the other hand, physical methods are generally easy and inexpensive, but the enzymes may have a low activity. No immobilization technique is right for all enzymes and all applications. Each case must be considered individually to determine which immobilization method is suitable for the enzyme and application.

Entrapment in hollow fibers is a physical method of immobilization which has many advantages. Preparation is simple, and the enzymes generally retain most of their activity. Enzymes may be easily co-immobilized with other enzymes or co-factors. In addition, enzymes and fibers may be recovered and re-used.

In this work, enzymes have been entrapped in hollow fibers. Hollow fibers are extruded from several types of polymers and consist of three regions: lumen, ultrathin skin, and macroporous or spongy region. A cross-section of a hollow fiber is shown in

Figure 2.1. The macroporous region is 80 - 90% void, has a large hydraulic permeability, and is the support structure for the fiber [15]. The ultrathin skin has small pores and serves as a barrier to molecules which cannot fit through the pores. The size of the pores is determined by the extrusion process and is classified by molecular weight cutoff.

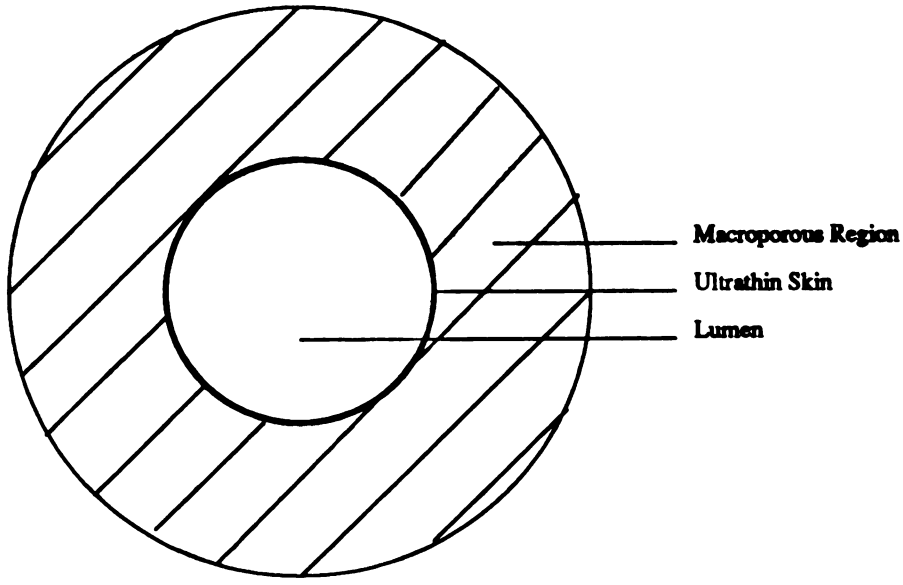

Figure 2.1. Cross-Section of a Hollow Fiber

An enzyme can be immobilized in the macroporous region. The ultrathin skin with a suitable molecular weight cutoff prevents the enzyme from diffusing from the macroporous region through the ultrathin skin to the lumen; however, the substrate for the enzyme is generally small and can pass through the ultrathin skin easily. It is not known whether the enzyme is simply trapped in the macroporous region or is reversibly adsorbed to the polymer, although work by Reiken suggests that adsorption probably does occur [20].

Three modes of flow regimes exist for the hollow fiber reactor: ultrafiltration, backflush, and recycle. Figure 2.2 illustrates these modes of flow. For ultrafiltration, the fluid is forced from the lumen through the ultrathin skin and macroporous region. This is the mode in which hollow fibers are traditionally used for separations. Backflush is the reverse of this: fluid flows from the macroporous region through the ultrathin skin to the lumen. For recycle, the fluid flows through the lumen, and the substrate diffuses through the ultrathin skin into the macroporous spongy region where it reacts with the enzyme, and the reaction product then diffuses back into the lumen. Ultrafiltration is commonly used to remove enzyme from a fiber, recycle is used for the reactor, and backflushing is used to load the fiber with the enzyme or to run a reactor. When used as a reactor, backflushing has several advantages over recycle. In backflush mode, the substrate is carried by convection to the enzyme, whereas in the recycle mode the substrate must rely on diffusion for transport to the enzyme. The fluid flow also prevents the enzyme from diffusing out of the macroporous region because the direction of flow is toward the ultrathin skin, so the enzyme is forced against a membrane which it cannot penetrate. In recycle, the enzyme is free to diffuse. In practice, the enzyme in a recycle reactor migrates from the upstream end to the downstream end due to pressure differences [16].

Resistance to flow is much greater for the backflush reactor. The ultrathin skin acts as a filter and has significant resistance to flow. In addition, the enzyme and impurities act as a filter cake and further impede flow. The total resistance of the reactor, R_T, can be divided into two parts: the resistance due to the fiber itself, R_f, and the resistance due to the enzyme, R_e, as shown in the following equation :

$$R_T = R_f + R_e \tag{2.12}$$

The resistance of the fiber is constant and is specific to the fiber. The resistance due to the enzyme is dependent on the specific enzyme and its concentration. A more detailed discussion of the immobilization characteristics of the enzyme will be provided Chapter

4. In the following section, a discussion of the mathematical model used for enzymatic catalysis of recycle HFERs is provided.

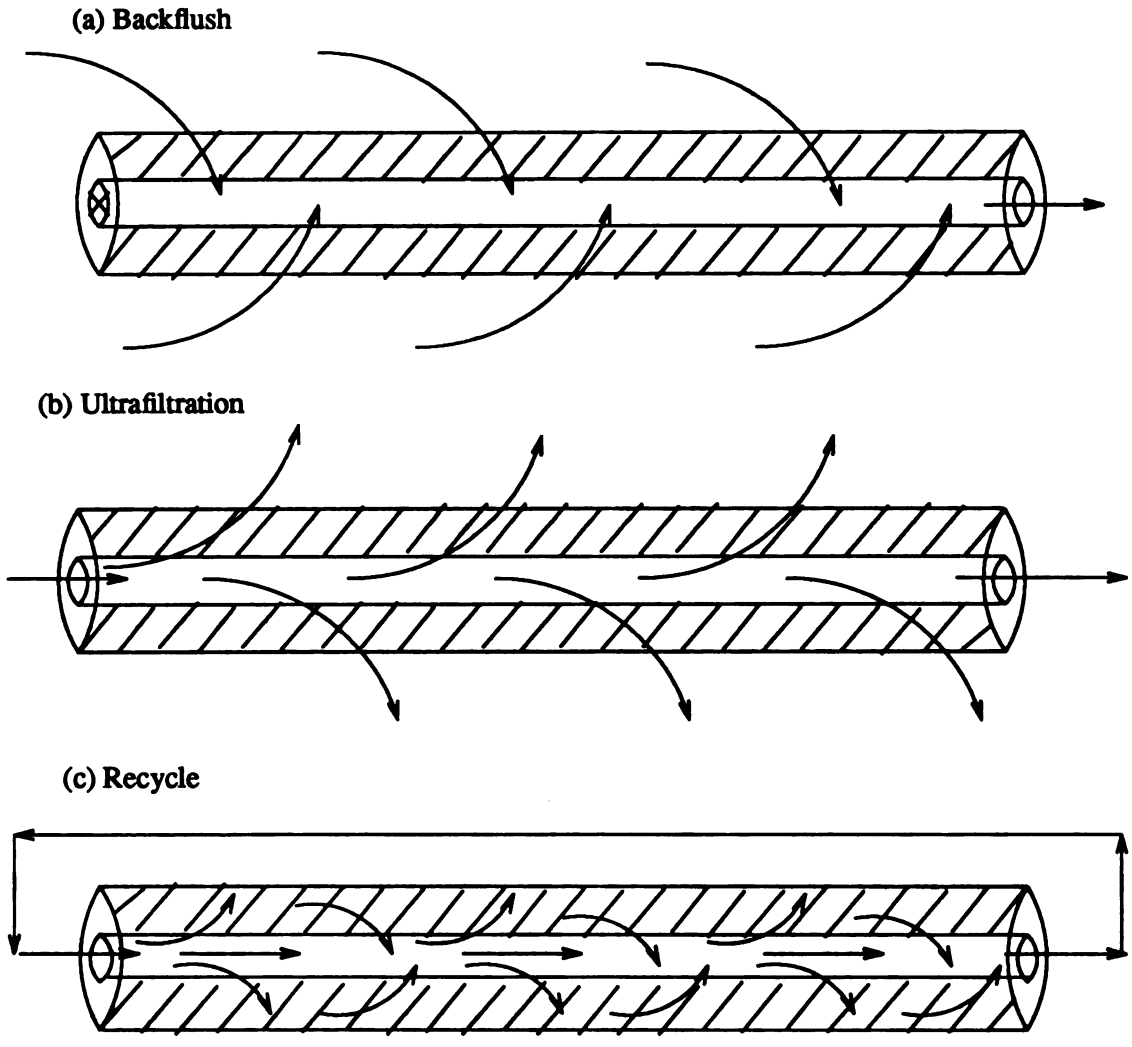

Figure 2.2. Modes of Flow

2.3 Mathematical Models for Recycle HFERs

Of the three modes of flow for hollow fiber reactors, recycle flow has been used most often. There have been many analyses of the flow and kinetics of recycle reactors. To determine intrinsic immobilized kinetics, which will be discussed in Chapter 4, the reactor is run in the recycle mode. Waterland *et al.* developed a mathematical model for

enzymatic catalysis of recycle HFERs [14]. The model was based on the general diffusion equation:

$$\frac{Dc}{Dt} = \mathbf{D}\nabla^2 c + R \tag{2.13}$$

where c is the concentration of substrate, **D** is the diffusion coefficient, and R is the reaction rate. This equation holds for each region of the fiber. Therefore, when it is simplified for the HFER, Equation (2.1) becomes:

$$\mathbf{D_s}\frac{1}{r}\frac{\partial}{\partial r}(r\frac{\partial c_s}{\partial r}) = R_s \tag{2.14}$$

for the sponge region,

$$\mathbf{D_m}\frac{1}{r}\frac{\partial}{\partial r}(r\frac{\partial c_m}{\partial r}) = 0 \tag{2.15}$$

for the ultrathin membrane, and

$$\mathbf{D_l}\frac{1}{r}\frac{\partial}{\partial r}(r\frac{\partial c_l}{\partial r}) = v_z\frac{\partial c_l}{\partial z} \tag{2.16}$$

for the lumen. For these equations $\mathbf{D_s}$, $\mathbf{D_m}$, $\mathbf{D_l}$ are the diffusion coefficients for the sponge, ultrathin membrane, and lumen regions, respectively; c_s, c_m, c_l are the concentrations for each region; and v_z is the axial fluid velocity in the lumen.

The boundary conditions for these equations are

$$\frac{\partial c_s}{\partial r}\Big|_{r=r_s} = 0 \tag{2.17}$$

$$\gamma c_s|_{r=r_m} = c_m|_{r=r_m} \tag{2.18}$$

$$\mathbf{D_s}\frac{\partial c_s}{\partial r}\Big|_{r=r_m} = \mathbf{D_m}\frac{\partial c_m}{\partial r}\Big|_{r=r_m} \tag{2.19}$$

$$c_m|_{r=r_l} = \gamma c_w(z) \tag{2.20}$$

$$\mathbf{D_m}\frac{\partial c_m}{\partial r}\Big|_{r=r_l} = \mathbf{D_l}\frac{\partial c_l}{\partial r}\Big|_{r=r_l} \tag{2.21}$$

$$c_l|_{r=r_l} = c_w(z); \quad z>0 \tag{2.22}$$

$$c_l = c_0; \quad z<0 \tag{2.23}$$

$$\frac{\partial c_l}{\partial r}|_{r=0} = 0 \tag{2.24}$$

where r_s is the radial distance to the outside edge of the spongy region, r_m is the radial distance to the interface between the spongy region and the ultrathin membrane, r_l is the radial distance to the interface between the ultrathin membrane and the lumen, γ is the partition coefficient for the ultrathin membrane, c_w is the concentration at $r = r_l$, and c_0 is the concentration at the inlet. This set of equations can be solved analytically when the reaction rate follows first order kinetics. Most enzyme reactions, however, follow the more complicated Michaelis-Menten kinetics which can be described by the following equation

$$R = \frac{v_{max}c}{K_m + c} \tag{2.25}$$

where R is the rate of reaction, v_{max} is the maximum rate, c is the concentration of substrate, and K_m is the Michaelis-Menten constant. For these more complicated kinetics, Equations (2.14-16) cannot be solved analytically, but numerical techniques have been developed for approximate solutions for this case [14,17].

Webster and Shuler also developed a model for hollow fiber reactors [18]. Although they considered whole cell reactors rather than enzymes, the model equations are the same (Equations (2.14-16)). Webster and Shuler also neglected resistances to mass transfer in the ultrathin skin and lumen, and thus Equations (2.15) and (2.16) were neglected. The reaction rate was assumed to follow Michaelis-Menten kinetics. Equation (2.14) was solved for the zero-order and first-order limits of the Michaelis-Menten rate expression, and complex equations for the appropriate effectiveness factors were given. The effectiveness factor is defined as the ratio between the observed rate of reaction and

the reaction rate with no diffusion resistances. The system was also analyzed with the following unsteady-state mass balance:

$$\frac{V_s v_{max}[S]}{K_m + [S]} - Q[S_0]x = V_t \frac{d[S]}{dt} \tag{2.26}$$

which can also be expressed as

$$\frac{V_s v_{max} C_{A0}(1-x)}{K_m + C_{A0}(1-x)} - QC_{A0}x = V_t \frac{d([C_{A0}]x)}{dt} \tag{2.27}$$

The first term on the left-hand side represents the generation of product via the Michaelis-Menten kinetics, and the second term represents the rate of product removal by flow. The term on the right-hand side accounts for the accumulation in the system. Webster and Shuler solved this equation for the transient concentration of substrate.

Moo-Young and Kobayashi developed expressions for effectiveness factors for Michaelis-Menten kinetics [19]. They considered both uninhibited and inhibited forms of the rate expression. This analysis was used to determine immobilized enzyme kinetic constants for glutamate oxidase immobilized in a HFER.

2.4 Mathematical Models for Backflush HFERs

The HFER has two main disadvantages when run in the recycle mode. First, the recycle HFER has significant mass transfer resistance due to diffusion when run under normal conditions [20]. Second, there is axial transport in the sponge region caused by the pressure drop in the lumen [15,16]. The higher pressure at the inlet causes ultrafiltration for the upstream half of the reactor and backflushing for the downstream half. This causes the enzyme or cells to migrate from the first half of the reactor towards the end of the reactor. Since there is a higher concentration of cells or enzymes at the end

of the reactor where the substrate concentration is the lowest, the overall rate of reaction is lower. To avoid this problem, the reactor should be run in the diffusion-controlled regime [15].

These problems can be avoided by operating the reactor in backflush mode. Since the main mechanism of transport in backflush flow is convection, diffusion resistance contributes less. Also, the pressure is distributed evenly across the whole sponge region, and therefore axial diffusion in the sponge region would be minimized [16].

There are, however, two limitations to the backflush HFER [21]. First, the pressure drop and flow rate are limited by the burst strength of the membrane. More importantly, enzymes cannot withstand high pressures, so the burst strength of the fibers is not a major concern. Second, the feed must be of permeate quality to avoid fouling the hollow fiber. In most enzyme applications, however, the feed should be as pure as possible to avoid inhibiting or poisoning the enzyme and to simplify downstream separations. Consequently, the limitation that could result from potential fouling should be minimal.

Jones *et al.* developed a reactor which ran solely in the backflush mode [21]. Their reactor consisted of a cartridge of hollow fibers. They designed an immobilization procedure which yielded high enzyme loadings and thus high substrate conversions, and they evaluated the performance of the reactor. A mathematical model for the reactor was developed. In developing this model, they made several assumptions. The fibers were assumed to be in an equilateral triangular array. The reactor was assumed to be at steady state and have constant shell-side pressure and constant temperature. The fluids were assumed to be Newtonian and to obey the Hagen-Pouseuille equation in the lumen. They assumed uniform substrate concentration in the shell, no adsorption of substrate or product in the macroporous region, and negligible axial dispersion. They also assumed that the intrinsic kinetics of the enzyme were unaffected by immobilization.

The last assumption was a poor one because intrinsic kinetics are indeed affected by immobilization. Reiken, Knob and Briedis developed a procedure to estimate immobilization kinetics and found that the kinetic constants do change [22]. Simple corrections could be made to the model's parameters to incorporate the effect of immobilization. The assumption of constant shell-side pressure was verified by Tharakan and Chau [16]. The other assumptions are reasonable for the conditions of the reactor.

Jones *et al.* first developed an equation for the velocity of fluid in the fiber. The radial velocity at the wall was found to be

$$v_{rw}(z) = \frac{-A\,\Delta P \cosh(\frac{\beta z}{l})}{\cosh\beta + (\frac{l_s}{l})\beta\sinh\beta} \tag{2.28}$$

where A is the membrane coefficient, ΔP is the pressure difference between the inlet and outlet, β is a constant based on the hollow fiber properties, z is the axial direction, l is the hollow fiber length, and l_s is the fiber epoxy seal length. Because this equation was a function of the axial direction, z, an equation for the corresponding mean radial wall velocity between z_1 and z_2 was also developed.

$$\bar{v}_{rw} = \frac{-\frac{Al}{\beta}\Delta P\left[\sinh\left[\frac{\beta z_2}{l}\right]-\sinh\left[\frac{\beta z_1}{l}\right]\right]}{\left[\cosh\beta + \left[\frac{l_s}{l}\right]\beta\sinh\beta\right](z_2-z_1)}, \quad l \geq z_2 \geq z_1 \geq 0 \tag{2.29}$$

Since the radial wall velocity is a weak function of axial position, it was assumed for the model that the radial wall velocity was constant. Hence, the concentration in the lumen could be assumed to be independent of axial position. This allows the decoupling of the general mass balances (from Equation (2.13) written for substrate and product concentration in the sponge region) and leaves the following two ordinary differential equations:

$$\mathbf{D_s}\frac{d^2s}{dr^2} + \frac{1}{r}(\mathbf{D_s} - v_{rw}r_0)\frac{ds}{dr} - f(s,p) = 0 \tag{2.30}$$

$$\mathbf{D_p}\frac{d^2p}{dr^2} + \frac{1}{r}(\mathbf{D_p} - v_{rw}r_0)\frac{dp}{dr} + f(s,p) = 0 \tag{2.31}$$

where $\mathbf{D_s}$ and $\mathbf{D_p}$ are the diffusion coefficients of the substrate and product, respectively, s is the substrate concentration, p is the product concentration, r_0 is the outer fiber radius, and $f(s,p)$ is the reaction rate. In this case, $f(s,p)$ was the Michaelis-Menten rate equation and had the form

$$f(s,p) = \frac{kEs}{K_m + s + p\frac{K_m}{K_I}} \tag{2.32}$$

where k is the rate constant, E is the total enzyme concentration, s is the substrate concentration, K_m is the Michaelis-Menten constant, p is the product concentration, and K_I is the product inhibition constant. Using the dimensionless variables $s^* = \frac{s}{s_s}$, $p^* = \frac{p}{s_s}$, and $x = \frac{(r-r_i)}{(r_0-r_i)}$ (where s_s is the substrate concentration in the shell, r_i is the inner fiber radius, and r_o is the outer fiber radius), Equations (2.30) and (2.31) become:

$$\frac{d^2s^*}{dx^2} + \gamma(x)Pe_{1s}\frac{ds^*}{dx} - \Omega_s\frac{s^*}{\frac{K_m}{s_s} + s^* + p^*\frac{K_m}{K_I}} = 0 \tag{2.33}$$

$$\frac{d^2p^*}{dx^2} + \gamma(x)Pe_{1p}\frac{dp^*}{dx} + \Omega_p\frac{s^*}{\frac{K_m}{s_s} + s^* + p^*\frac{K_m}{K_I}} = 0 \tag{2.34}$$

The boundary conditions for these equations are:

$$\frac{ds^*}{dx}\Big|_{x=0} = 0 \tag{2.35}$$

$$\frac{dp^*}{dx}\Big|_{x=0} = 0 \tag{2.36}$$

$$\frac{ds^*}{dx}|_{x=1} = -Pe_{2s}(1-s^*) \tag{2.37}$$

$$\frac{dp^*}{dx}|_{x=1} = -Pe_{2p}(\frac{P_s}{s_s}-p^*) \tag{2.38}$$

From this analysis, four Peclet numbers (Pe_{1s}, Pe_{1p}, Pe_{2s}, Pe_{2p}) and three other dimensionless groups ($\gamma(x)$, Ω_s, Ω_p) were determined as follows:

$$Pe_{1s} = (1-\frac{v_{rw}r_o}{\mathbf{D_s}}) \tag{2.39}$$

$$Pe_{1p} = (1-\frac{v_{rw}r_o}{\mathbf{D_p}}) \tag{2.40}$$

$$Pe_{2s} = (\frac{v_{rw}(r_o-r_i)}{\mathbf{D_s}}) \tag{2.41}$$

$$Pe_{2p} = (\frac{v_{rw}(r_o-r_i)}{\mathbf{D_p}}) \tag{2.42}$$

$$\gamma(x) = \frac{(r_o-r_i)}{x(r_o-r_i)+r_i}) \tag{2.43}$$

$$\Omega_s = \frac{kE(r_o-r_i)^2}{\mathbf{D_s}x_l} \tag{2.44}$$

$$\Omega_p = \frac{kE(r_o-r_i)^2}{\mathbf{D_p}x_l} \tag{2.45}$$

If the diffusion coefficients of the substrate and the product have the same value, the substrate and product concentrations can be related by

$$s^* + p^* = 1 + \frac{p_s}{s_s} \tag{2.46}$$

Using this relation, only one governing Equation (2.33) or (2.34) need be solved.

For the more complex case where the radial wall velocity is not independent of axial position, a more complex model must be developed. Jones *et al.* treated the HFER as a series of compartments as shown in Figure 2.3. In each compartment, the radial wall

velocity was taken to be constant and the Equations (2.33) and (2.34) to apply. However, the boundary conditions were different for each compartment. To determine the boundary conditions, Jones *et al.* adopted a model that is shown in Figure 2.4. This model accounts for radial dispersion between the lumen and sponge. Each compartment can be represented by a stirred tank connected to a plug flow reactor (PFR) which is connected to another stirred tank. The first stirred tank represents the well-mixed shell region of the reactor, and the PFR represents the sponge region of the fiber. The second stirred tanks of each compartment are connected in series and collectively form the lumen. The collection of stirred tanks in series represents plug flow in the lumen without axial dispersion.

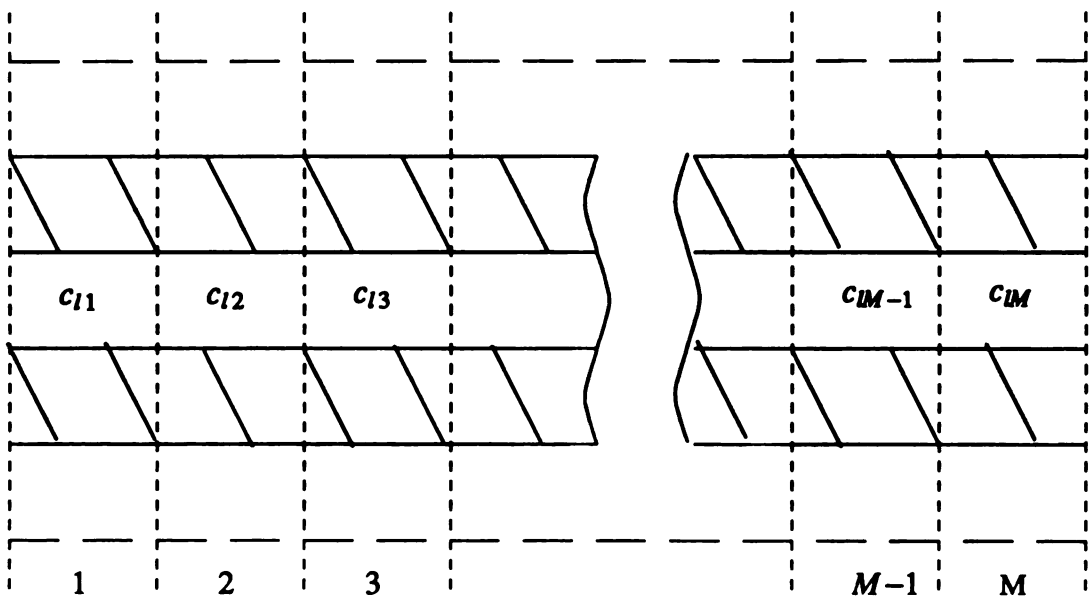

Figure 2.3. Compartmental Model of a Backflush HFER

The solution of this model for concentration as a function of position can be obtained by solving Equations (2.33) and (2.34). However, two of the boundary conditions for these equations differ for this representation of the reactor. Equations (2.37) and (2.38) remain the same, but Equations (2.35) and (2.36) become:

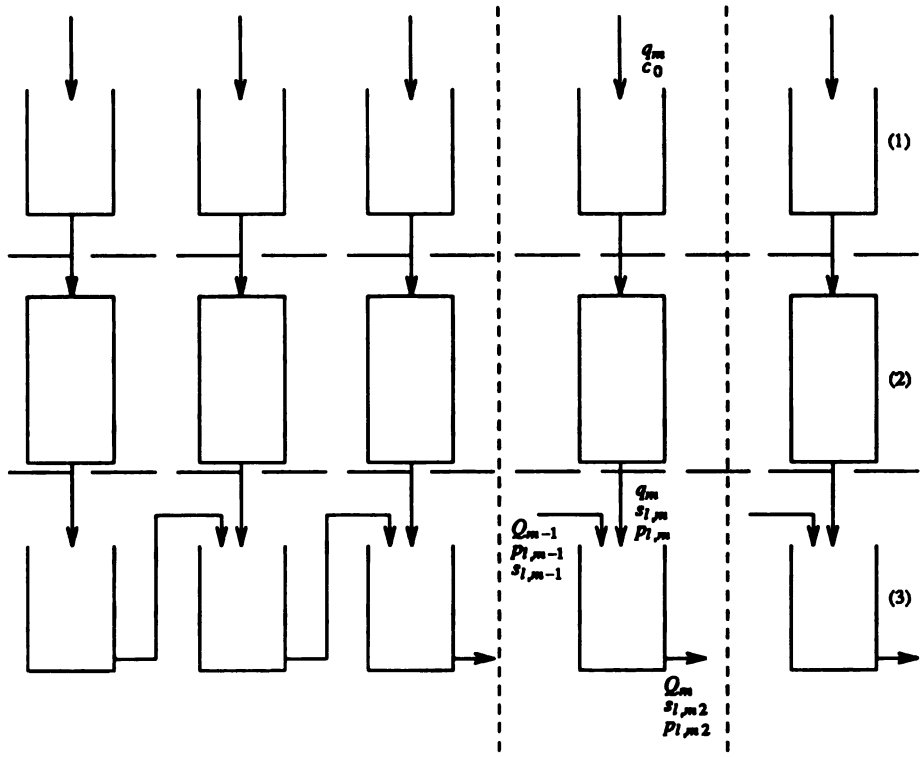

(1): Shell (Stirred Tanks)

(2): Spongy Region (PFRs)

(3): Lumen (Stirred Tanks)

Figure 2.4. Model for Backflush HFER with Axial Dispersion

$$\frac{ds^*}{dx}|_{x=0} = -Pe_{3s}(\frac{s_{l,m-1}}{s_s} - s^*) \tag{2.47}$$

$$\frac{dp^*}{dx}|_{x=0} = -Pe_{3p}(\frac{p_{l,m-1}}{s_s} - p^*) \tag{2.48}$$

These two boundary conditions include two new Peclet numbers which are defined by

$$Pe_{3s} = \frac{Q_{m-1}(r_o - r_i)}{D_s X_l} \tag{2.49}$$

$$Pe_{3p} = \frac{Q_{m-1}(r_o - r_i)}{D_p X_l} \tag{2.50}$$

In these equations Q_{m-1}, $s_{l,m-1}$, and $p_{l,m-1}$ are shown in Figure 2.4. The variable X_l is the cross-sectional area at the lumen wall. Again, the solution for concentration distribution may be simplified if Equation (2.46) applies. In this case, only Equation (2.33) or (2.34) and their respective boundary conditions need to be solved.

2.5 Characterization of Glutamate Oxidase

The enzyme used in this project was glutamate oxidase. It was discovered by Kusakabe *et al.* by isolation from the *actinomycetes* strain X-119-6 [1]. It has a molecular weight of 140,000 and consists of three subunits. The molecular weights of the subunits, α, β, and γ are 44,000, 19,000 and 9000, respectively. This led to the molecular formula $\alpha_2\beta_2\gamma_2$. Two molecules of FAD are bound to each glutamate oxidase molecule.

The enzyme catalyzes the oxidative deamination of glutamate.

$$glutamate + O_2 + H_2O \longrightarrow \alpha\text{–}ketoglutarate + NH_3 + H_2O_2 \qquad (2.50)$$

One unit of glutamate oxidase is defined as the amount which consumes 1 μmole of O_2 per minute in the absence of catalase. Glutamate oxidase is very specific for glutamate. Its K_m for glutamate is 0.21 mM and for L-aspartic acid, its K_m is 29 mM. No other amino acids are oxidized by glutamate oxidase. At pH 7.4, L-aspartic acid is oxidized to 0.6% while glutamate is oxidized to 100%. When the pH is lowered to 6.0, glutamate oxidation remains at 100%, but the oxidation of aspartic acid decreases to less than 0.1%.

Glutamate oxidase remains active over a wide pH range. It has at least 50% activity from pH 4.0 to pH 10.0. Its maximum reactivity is in the pH range of 7.0 to 8.0, and its isoelectric point is at pH 6.2. Glutamate oxidase is thermostable in the pH range 5.5 to 6.5. At pH 5.5 it is stable for 15 minutes at 65 °C. After 15 minutes at 75 °C, the glutamate oxidase retains 87% of its activity. Even at 85 °C, it retains 47% of its activity after

15 minutes. Glutamate oxidase has very few inhibitors. The only significant inhibitor tested by Kusakabe *et al.* was 1 mM p-chloromercuribenzoate.

Chapter 3

Methods of Analysis

The purpose of this project was to develop a biosensor to detect glutamate. To evaluate the performance of the sensor, accurate methods to measure concentration of enzyme and extent of reaction were needed. Due to the recent discovery of the enzyme glutamate oxidase, consistent and accurate assays were difficult to find.

The purpose of this chapter is to describe the methods and techniques used to prepare the hollow fiber backflush biosensor.

3.1 Protein Assay

Since glutamate oxidase is a protein, a protein assay is convenient for measuring the concentration of glutamate oxidase. The specification information provided with the glutamate oxidase indicated that the glutamate oxidase was essentially free from other protein contaminants. The most common protein assay is the Lowry assay [23]. However, the Lowry assay gave inconsistent results for glutamate oxidase. The Lowry assay is sensitive to counterions and to the protein itself [24]. The enzyme solution may have contained an interfering ion, or glutamate oxidase may not be suitable for the Lowry assay.

Direct visible spectroscopy is another common protein assay. Proteins have absorption maxima in the 285-315 nm range. This assay is very simple since no chemical steps are required. However, the potassium phosphate used to buffer the enzyme solution

absorbs strongly in this range of frequencies. Also, the concentration of enzyme was very low so detection would be difficult. When potassium phosphate buffer (KPB) was used as the blank, the concentration of enzyme could not be measured accurately.

The protein assay bicinchoninic acid (BCA) is similar to the Lowry assay but is not as sensitive to reaction conditions as the Lowry assay. The BCA assay gave consistent, accurate results. The assay kit was purchased from Pierce Chemical (Rockford, Illinois). The kit consists of two reagents, A and B. Reagent A is a solution of sodium carbonate, sodium bicarbonate, BCA detection reagent, and tartrate in 0.1N sodium hydroxide. Reagent B is a 4% solution of $CuSO_4 5H_2O$. One part of Reagent B was mixed with 50 parts Reagent A to make the working solution. The working solution was prepared fresh for each assay. Four milliliters (ml) of the working solution were mixed with 0.2 ml of the sample. The sample and working solution mixtures were then incubated at 30 °C for 30 minutes or at room temperature for two hours or overnight. The absorbance of each sample was measured at 562 nm using a Perkin Elmer Lambda 3A Spectrophotometer. The samples were measured against a blank of 4 ml of working solution and 0.2 ml of KPB.

The amount of glutamate oxidase was determined by comparing the absorbance of the sample with a calibration curve. The calibration curve was developed by measuring the absorption of bovine serum albumin (BSA) solutions in the concentration range of 0-300 mg/ml. The absorbance of a given concentration of BSA changed slightly for different working solutions, so a new calibration was performed for each assay. The calibration curves were generally very straight, with linear regression correlation constants of 0.98 or better. The reading of the concentration was performed accurately. When the sample concentration was expected to be low, 30 mg of BSA was added to the sample. The addition of the BSA brought the concentration into a range that could be read more accurately.

3.2 Preparation of the Enzyme

The glutamate oxidase was donated by Yamasa Shoyu Co., Ltd. of Japan and came freeze dried in a base of lactose and KPB at pH 7.4. To prepare the enzyme for use, the enzyme powder was dissolved in doubly distilled, (DD), water and placed in dialysis tubing with a molecular weight cutoff (MWC) of 10,000. The solution was dialyzed against pH 7.4 KPB for 24 hours. The enzyme was then stored in a refrigerator at 10°C until use.

3.3 Preparation of the Reactor

The reactor used in these experiments is shown in Figure 3.1. The hollow fiber was encased in a glass tube. Tygon tubing was clamped to all four ports. The hollow fiber was cemented to Luer fittings with epoxy which held the hollow fiber in place.

The reactor was cleaned and disinfected before each use. First, phosphoric acid at pH 3.0 was pumped through the shell and lumen for 30 minutes each. Then doubly distilled water was pumped through each side for 5 minutes. The procedure was repeated with 2.5 N NaOH and then rinsed for 10 minutes with DD water. Because microorganisms had been observed growing on the inside and outside of the hollow fiber, the reactor was washed with a solution of Tergizyme (Fischer Scientific). The Tergizyme consists of proteolytic enzymes and detergent. The Tergizyme was dissolved in warm (50°C) DD water according to package directions. The solution was pumped through each side for one hour. Each side was rinsed twice with fresh DD water for 15 minutes. To deactivate any proteolytic enzymes that might have remained, the reactor was again cleaned with phosphoric acid. In addition to cleaning both sides (shell and lumen), the reactor was ultrafiltered with phosphoric acid to flush any debris from the sponge region. The fiber was rinsed by ultrafiltering DD water for 20 minutes. As a preparation for storage, both sides of the reactor were rinsed with 10 ppm bleach solution for 20 minutes on each side. Before use, each side of the reactor was rinsed with DD water for 20 minutes followed by

ultrafiltering KPB for 5 minutes.

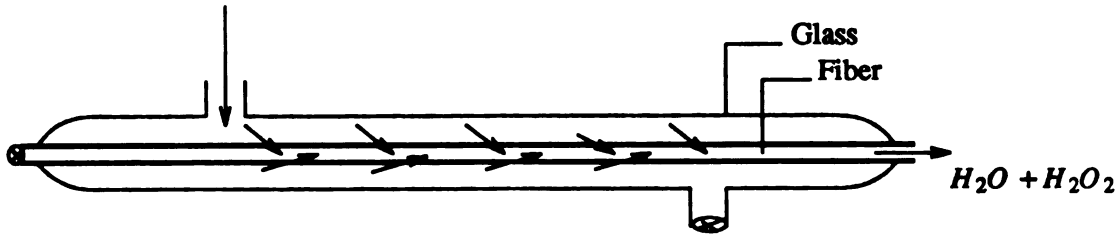

Figure 3.1 Single Fiber Reactor Operation

3.4 Loading the Reactor

To load the reactor, an enzyme solution was forced from the shell-side to the lumen which trapped the glutamate oxidase in the pores of the sponge region of the hollow fiber. Since this is similar to backflushing, this loading method is called backflush loading. First a 40 ml syringe was filled with the desired amount of glutamate oxidase solution and placed in a syringe pump. A cleaned and rinsed reactor was attached to the syringe at one of the shell-side ports. The other shell-side port was left open to allow the shell to fill evenly. One of the lumen ports was clamped shut, and the syringe pump was turned on. Once the shell was filled, the pump was turned off, and the open shell side port was clamped shut. The pump was turned on again, and the effluent from the lumen was collected for analysis by BCA protein assay.

3.5 Determination of the Extent of the Reaction

An assay for the detection of extent of the reaction for glutamate was difficult to find. The reaction was

$$glutamate + O_2 + H_2O \longrightarrow \alpha\text{–}ketoglutarate + NH_3 + H_2O_2 \qquad (3.1)$$

Since the reaction was aqueous, five of the compounds had potential for assay techniques. The first assay attempted was for α-ketoglutarate. The assay uses saccharopine dehydrogenase to catalyze the following reaction

$$lysine + \alpha\text{–}ketoglutarate + NADH + K^+ \rightleftharpoons saccharopine + NAD^+ + H_2O \qquad (3.2)$$

This reaction is reversible, so an excess of one of the reactants is needed to force the reaction to completion. This assay was used with success in measuring lysine concentrations by adding a large excess of α-ketoglutarate and measuring the decrease in NADH concentration using a spectrophotometer [25,26]. To measure α-ketoglutarate, an excess of lysine was used. However, after assaying several samples, it was apparent that the results were not consistent. After consulting Sigma Chemical Co., the sole source of the enzyme saccharopine dehydrogenase, it was discovered that the saccharopine dehydrogenase preparation was contaminated with glutamate dehydrogenase. Glutamate dehydrogenase catalyzes essentially the reverse reaction of glutamate oxidase (Equation 3.1) but uses NADH as the electron donor. Since glutamate was present in the samples, it was impossible to determine how much of the decrease in NADH concentration was due to the saccharopine dehydrogenase reaction and how much was due to the glutamate dehydrogenase reaction. Thus, this assay was not used.

Keto acids are commonly assayed by the MBTH (3-methyl-2-benzothiazolinone hydrazone hydrochloride) technique [27,28,29,30]. MBTH reacts with any keto acid to form a product which has an absorption maximum in the range 300-350 nm. In the case of α- ketoglutarate, the absorption maximum was 320 nm. To prepare the sample for

assay, 2 ml of sample were added to 4 ml of 0.2 M KPB, pH 6.8. Then 1.6 ml of 0.1% MBTH solution were added, and the samples were incubated at 50 °C for 30 minutes. After cooling to room temperature, the samples were read in the uv-vis spectrophotometer at 320 nm against a blank.

This assay was used several times for samples with low glutamate concentration, and the results compared favorably to results found in the literature. However, the data were not consistent for samples with high glutamate concentrations. The assay was tested to determine if glutamate competed with α-ketoglutarate for the active site of MBTH. At low concentrations of glutamate, the interference was negligible, but at high concentrations of glutamate (greater than 2 mM), the interference was significant. Since some assays for the biosensor could be at high concentrations, this analytical technique could not be used.

Because of these problems, α-ketoglutarate was abandoned as the analyte for the reaction given in Equation (3.1). Glutamate was not a good choice either because most amino acid analyses are sensitive to ammonia which is a product of the reaction. High pressure liquid chromatography (HPLC) was an option, but the high cost and unavailability of equipment ruled this out. Oxygen is quite easy to measure with an oxygen electrode, but since the reactor was not air-tight, this method would be inaccurate. Hydrogen peroxide can also be measured with an electrode, but the method requires titration and is quite expensive. Ammonia can be easily measured with an ammonia electrode. The electrode is a gas-sensing electrode and is not sensitive to amino acids. Based on these considerations, the ammonia electrode was chosen as the analytical method.

An ORION ammonia electrode was purchased and prepared according to instructions. At pH 7.4 ammonia exists predominantly as ammonium ion (NH_4^+), and very little ammonia would be lost to the surroundings. However , the ammonia electrode is gas-sensing, so the ammonia must be in the non-ionic form. Sodium hydroxide was added to

the sample (2ml/100ml sample) to convert the ammonium ions to ammonia. The sample was read immediately to prevent loss of ammonia to the air. The voltage was read from a voltmeter and compared to a standard calibration. This method was very accurate and had a wide range of sensitivity.

Chapter 4

Experimental Results

This chapter describes the experiments conducted for the biosensor feasibility study. The enzyme glutamate oxidase was characterized in both free solution and immobilized on a hollow fiber. The response of the biosensor was tested and evaluated. Recommendations for improvements on biosensor design are also provided.

4.1 Free Solution Kinetics

Free solution intrinsic kinetics for glutamate oxidase were measured using initial rate data. Initial rates were obtained by adding glutamate oxidase to solutions of differing concentrations of glutamate. Ten test tubes were set up with glutamate concentrations ranging from 0 to 2.0 *mM*. The solutions were diluted with 0.1 M KPB pH 7.4 to reach a volume of 4.0 ml, and 0.5 units of glutamate oxidase was added. The reaction was allowed to run for one minute. The reaction was stopped with 0.3 ml of 5 M HCl which lowered the pH to 1.0. Before analysis, the pH was raised to 7.4 again by the addition of 0.6 ml of 2.5 M NaOH. The solutions were analyzed by the MBTH technique. It should be noted that glass test tubes were used for all samples because glutamate oxidase adsorbs to plastic.

Initial rates were calculated for each sample and used to determine the intrinsic Michaelis-Menten kinetic parameters, K_m and k. The parameters were estimated using a statistical technique developed by Wilkinson [31]. This technique weights the more reliable data points, obtained for high concentrations, and uses a non-linear regression method to estimate the kinetic constants. A computer program, which is described in Appendix A, was used to calculate the constants. The mean K_m value was 0.24 *mM* which agrees well with the value of 0.21 *mM* reported by Kusakabe *et al.* [1]. Kusakabe *et al.* did not report a k or v_m, and no other source in the literature reports these values for glutamate oxidase.

The K_m value is a measure of the affinity of the enzyme for the substrate with a low K_m indicating a strong affinity for the substrate. Since the K_m value of 0.24 for glutamate oxidase is fairly low, glutamate oxidase has a strong affinity for glutamate. The k or v_m value is the intrinsic kinetic rate constant for the enzyme where v_m is k multipled by the amount of enzyme. The k value of 0.144 *mM* is rather low, but when considered with the K_m value, the overall reaction rate is quite fast.

4.2 Immobilization Characteristics

Before proceeding with the design and testing of the biosensor, the immobilization characteristics of glutamate oxidase in hollow fibers were evaluated. First, the retention and activity of glutamate oxidase on various fibers were tested. The backflushed reactor was also tested for enzyme loss during operation.

Based on previous immobilization of similar enzymes, the fibers tested were PA10 (polyamide polymer with 10,000 MWC) and PM10 (polysulfone polymer with 10,000 MWC) [33]. Reiken found that PA30 and PM30 fibers (30,000 MWC) did not retain L-lysine-α-oxidase, an enzyme similar to glutamate oxidase, so these fibers were eliminated from consideration. The PM10 fibers retained glutamate oxidase slightly better

than the PA10 fibers. The PM10 fibers retained 60-89% of the glutamate oxidase when new fibers were used, whereas PA10 fibers retained approximately 40%. When the fibers were cleaned and reused, the enzyme retention increased to nearly 100% for both fibers. The retention advantage of new PM10 fibers coupled with the better availability of PM10 fibers led to the selection of PM10 fibers for the biosensor.

Since immobilization can alter the activity of an enzyme, glutamate oxidase was tested for changes in the activity. A PM10 fiber was ultrafiltered after it had been used once, and the effluent was assayed for protein with the BCA technique. The protein was assumed to be glutamate oxidase because no other protein contaminated the glutamate oxidase sample. The recovered protein was 85% of the original immobilized enzyme. The intrinsic kinetic constants were measured for this ultrafiltered sample of enzyme with the same initial rate experiments used to measure the kinetic constants of the fresh enzyme. Again, the Wilkinson statistical method was used to determine the kinetic constants, as described by the program in Appendix A. The K_m value decreased to 0.07 *mM* which indicates that the enzyme has a much stronger affinity for the substrate. However, the k value also decreased to 0.08 *mM* min^{-1} $unit^{-1}$ which indicates a decrease in the intrinsic rate constant. These changes can be explained by the effect of the immobilization procedure. The immobilization procedure and ultrafiltration changed the conformation of the enzyme and thus created a structure which caused the substrate to bind more easily. However this conformation change seemed to make the enzyme less efficient which caused the lower k value.

The fiber was also tested for retention of enzyme under backflush conditions. A clean, new PM10 fiber was loaded with glutamate oxidase and backflushed with 0.2 M KPB at pH 7.4 for 24 hours. The effluent was tested with the BCA technique for protein. The amount of protein which was lost from the fiber was less than 2%.

The PM10 fiber has high retention of glutamate oxidase, both from loading and during use as a backflush reactor, and glutamate oxidase recovered from PM10 fibers has an acceptable activity. Based on these results, we chose the PM10 fiber for use in the biosensor.

4.3 Pressure Drop

Before the fiber could be tested as a biosensor, the pressure drop characteristics of the fiber, especially the loaded fiber, needed to be determined. Pressure drop and the corresponding flow rates were measured for fibers. The glutamate oxidase loading ranged from clean fibers (zero glutamate oxidase) to 866 μgrams (23.6 units). Pressure drop was measured by Omega pressure transducers, and flow rates were measured by collecting the outlet flow from the reactor in a known time.

The flow rate through the fiber was limited by the pressure drop the fiber and enzyme can withstand. As discussed in Chapter 2, the maximum pressure drop over the fiber should be 10 psi. For a clean fiber, a 10 psi pressure drop yielded a flow rate of 0.8 ml/min, but the maximum flow rate for loaded fibers was 0.3 ml/min. This flow rate gives a superficial velocity of 4.87 μm/sec through the fiber which is twice the superficial velocity of 2.4 μm/sec reported by Jones *et al.* for their backflush reactor [21]. This difference, however, should not be surprising because their flow rate per fiber was lower.

The resistance of the fiber was determined by calculating the reciprocal of the slope of a plot of flow rate verses transmembrane pressure drop. This is shown in Figure 4.1. The resistances of fibers loaded with different amounts of enzyme were similar compared to the resistance of a clean fiber, as can be seen in Figure 4.2. Thus the resistances of loaded fibers can be grouped together to give an "average" resistance. The resistance of loaded fibers averaged 2.7 times the resistance of a clean fiber; the resistance of a clean fiber was 11.8 psi/(ml/min), and the resistance of loaded fibers was 31.6 psi/(ml/min).

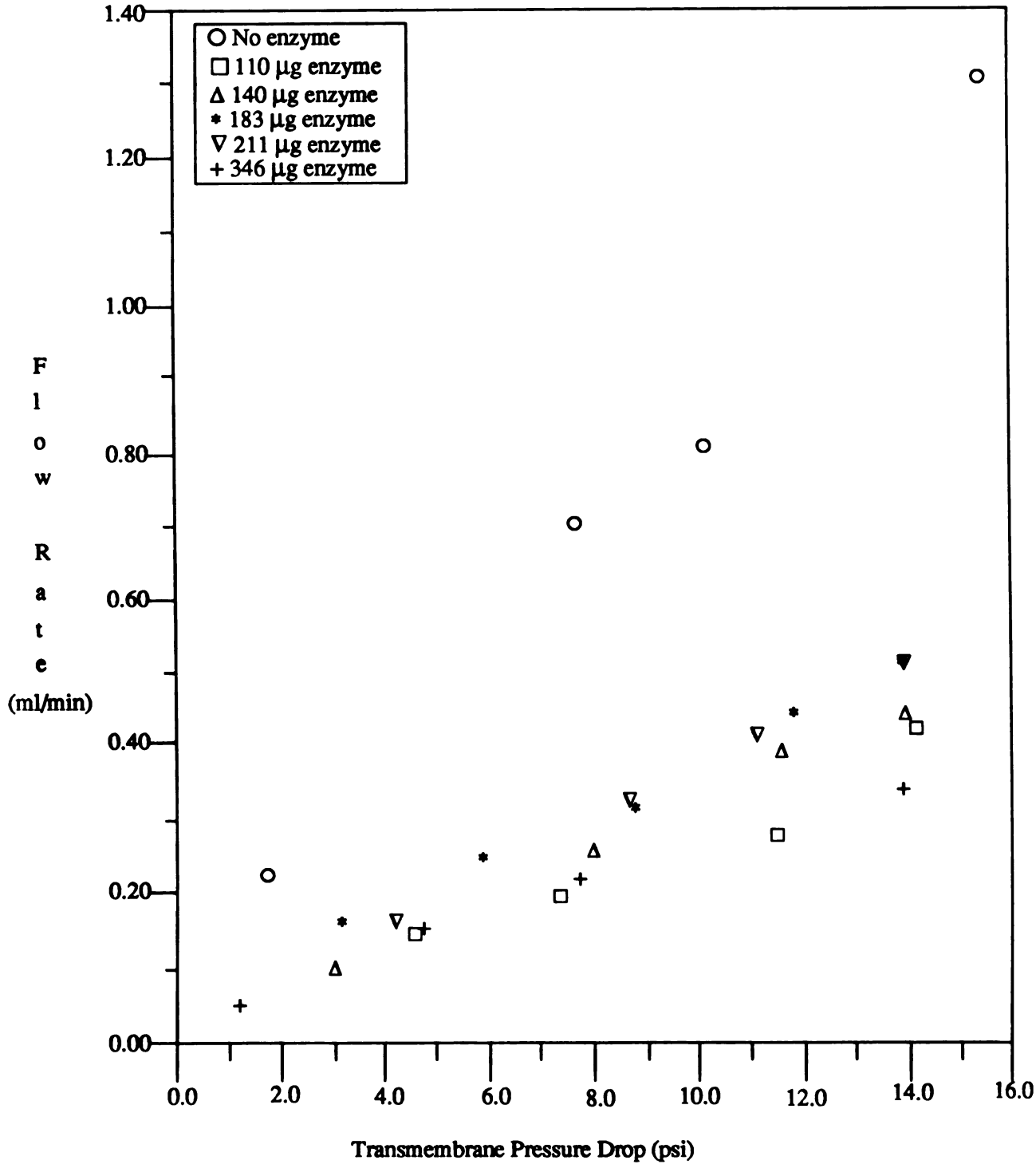

Figure 4.1. Effect of Enzyme Loading on Flow Rate and Transmembrane Pressure Drop

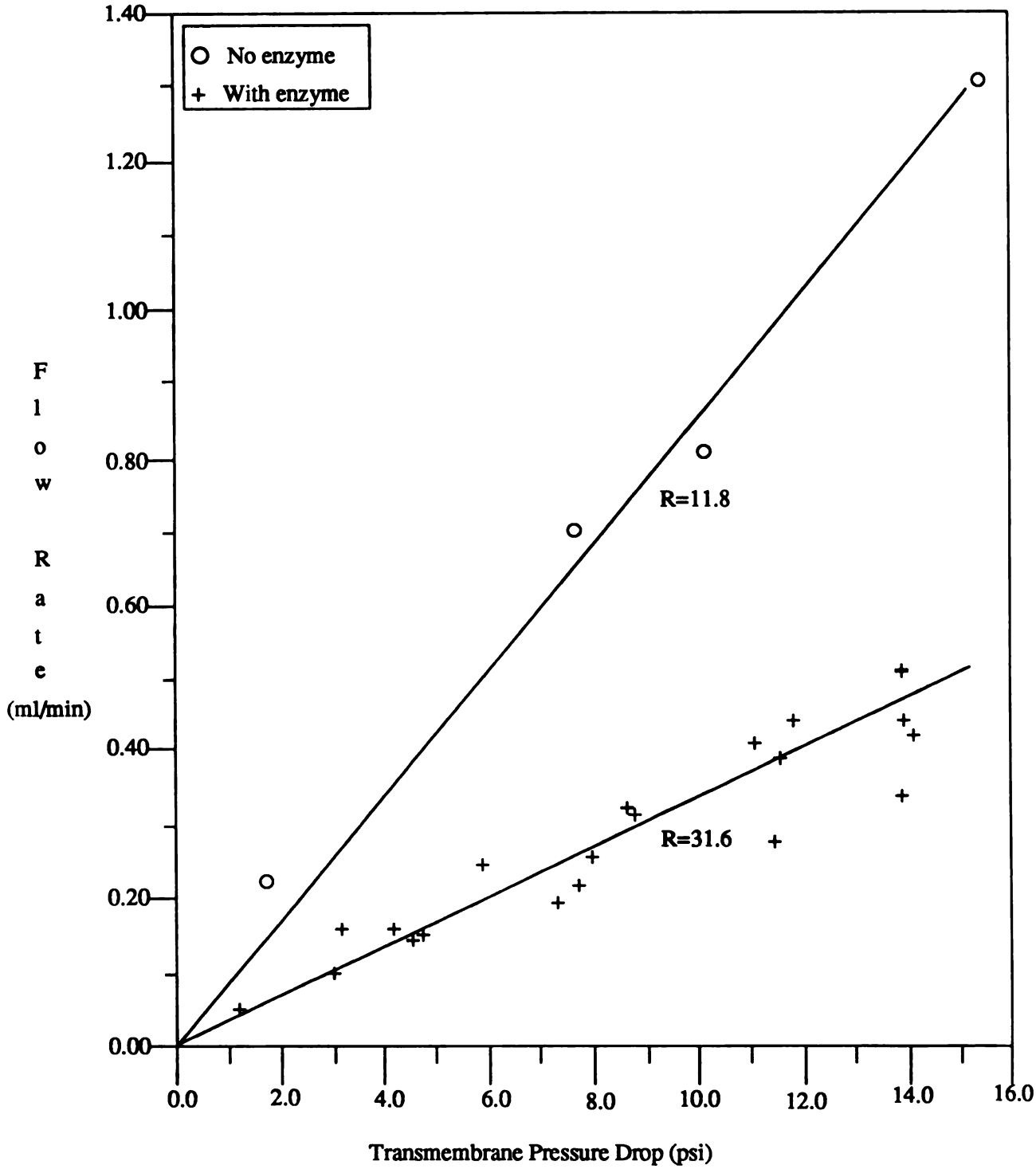

Figure 4.2. Comparison of Clean and Loaded Fibers

Therefore, the fiber itself accounts for 40% of the total resistance to flow. Upon closer examination, it was determined that the average resistance of several loaded fibers was directly proportional to enzyme loading and could be expressed by the following equation:

$$R = 0.0792m_e + 11.6 \tag{4.1}$$

where m_e is the mass of the enzyme and has the units of μgrams of glutamate oxidase.

The relationship between the mass of the enzyme loaded in the fiber and the resistance is shown in Figure 4.3. The constant in Equation (4.1) may be attributed to the fiber resistance. The regression value of 11.6 agrees well with the experimental value of 11.8 for a clean fiber. The proportionality of resistance to mass of enzyme may be attributed to the enzyme itself and may be quantified as $0.0792m_e$. This relationship can be explained by the assumption that the enzyme itself is blocking the pores of the sponge region. Increasing the amount of enzyme increases the number of pores that are blocked. Consequently, a greater resistance to flow is observed. It should be noted, however, that each fiber had different fiber and enzyme resistances. Equation 4.1 represents an average for all the fibers tested.

The permeability of the fiber and enzyme can be found from Darcy's Law:

$$\Delta P = K_T \eta \frac{Q}{A} \tag{4.2}$$

where ΔP is the pressure drop, K_T is a permeability constant, A is the cross-sectional area of flow, η is the fluid viscosity, and Q is the flow rate [32]. By rewriting the permeability constant K_T as two constants, K_f and K_e, which represent the contributions to the permeability of the fiber and enzyme, respectively, we get

$$\Delta P = (K_f + K_e)\eta \frac{Q}{A} \tag{4.3}$$

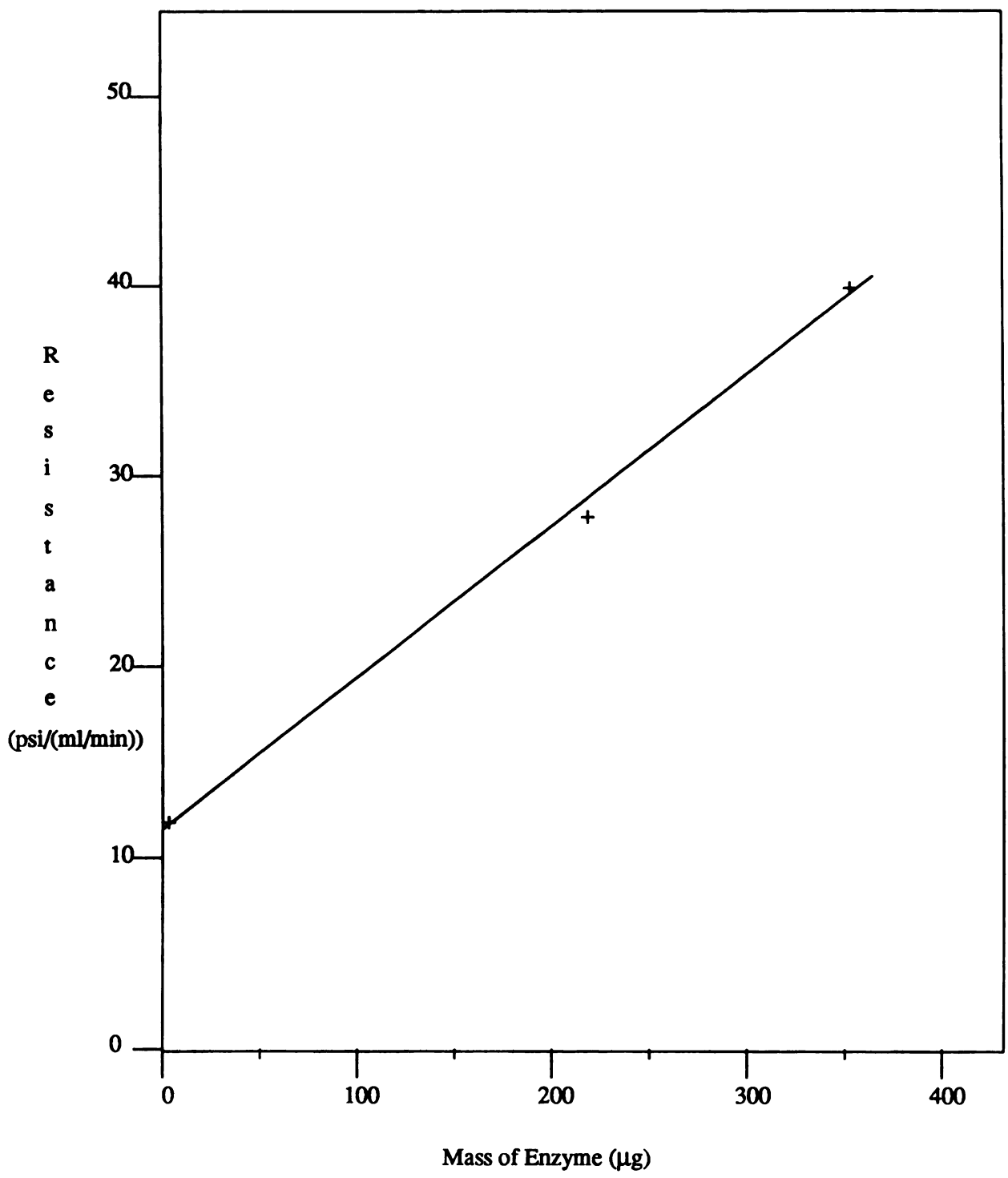

Figure 4.3. Resistance as a Function of the Mass of Enzyme Loaded on the Fiber

Since $\Delta P = R_T Q$,

$$R_T = (K_f + K_e)\frac{\eta}{A} \tag{4.4}$$

Dividing the total resistance into fiber resistance, R_f and enzyme resistance, R_e, Equation (4.4) becomes:

$$R_f = \frac{K_f \eta}{A} \tag{4.5}$$

$$R_e = \frac{K_e \eta}{A} \tag{4.6}$$

Assuming the viscosity is that of pure water, $1cP$, and using the ID of $1.118mm$ to calculate the area, this gives a value of $1.07 \times 10^8\ cm^{-1}$ for the permeability of the fiber and $1.78 \times 10^8\ cm^{-1}$ for the average permeability of the enzyme. Since the resistance due to glutamate oxidase actually depended on the mass of enzyme immobilized on the fiber, the permeability due to glutamate oxidase also depended on the mass of immobilized glutamate oxidase. Using Equations (4.1) and (4.6) and solving for K_e gives

$$K_e = 7.15 m_e \tag{4.7}$$

where m_e again has the units of micrograms.

4.4 Characteristics of the Glutamate Oxidase Backflush HFER

The biosensor was first tested as a reactor to determine the optimum operating parameters. The reactor was run in the backflush mode with a maximum transmembrane pressure drop of 10 psi. The outlet ammonia concentration was measured as a function of glutamate concentration and enzyme loading.

The reactor was tested for response to different glutamate concentrations. A clean reactor was loaded with 366 μg (10 units) of glutamate oxidase. The effluent from the reactor was returned to the reservoir as shown in Figure 4.4. The reactor was run for

approximately 3 hours. A 1.5 ml sample was withdrawn approximately every 30 minutes. The samples were analyzed for ammonia concentration with the ammonia electrode.

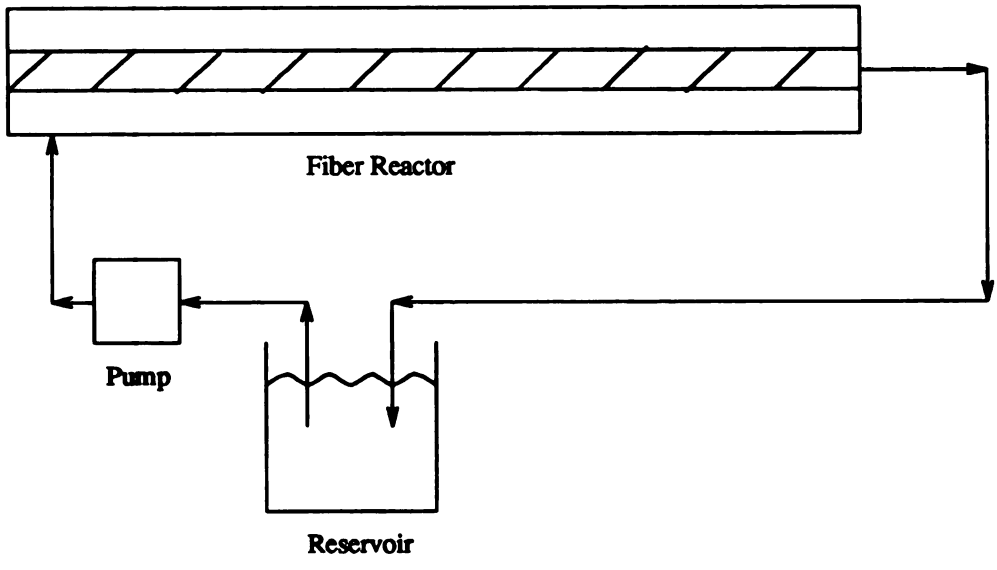

Figure 4.4. Schematic of Backflush Recycle Reactor

The two glutamate concentrations tested were 2 *mM* and 5 *mM*. The results are shown in Figure 4.5. The concentration of ammonia rose somewhat faster for the 5 *mM* glutamate solution than for the 2 *mM* solution. As expected, when the glutamate concentration was higher, the reaction was more rapid. This result indicates that the biosensor should be able to differentiate between glutamate concentrations.

The reactor response was also tested for different enzyme loadings. The reactor was run as in the previous experiment except that only the 5*mM* glutamate solution was used. The reactor was first loaded with 210 μg (5.7 units) of glutamate oxidase. Then the loading was increased to 366 μg (10 units). The results of this experiment are shown in Figure 4.6. The reactor with the higher enzyme concentration had a higher fractional conversion. This is as expected because as the amount of enzyme increases, there is more

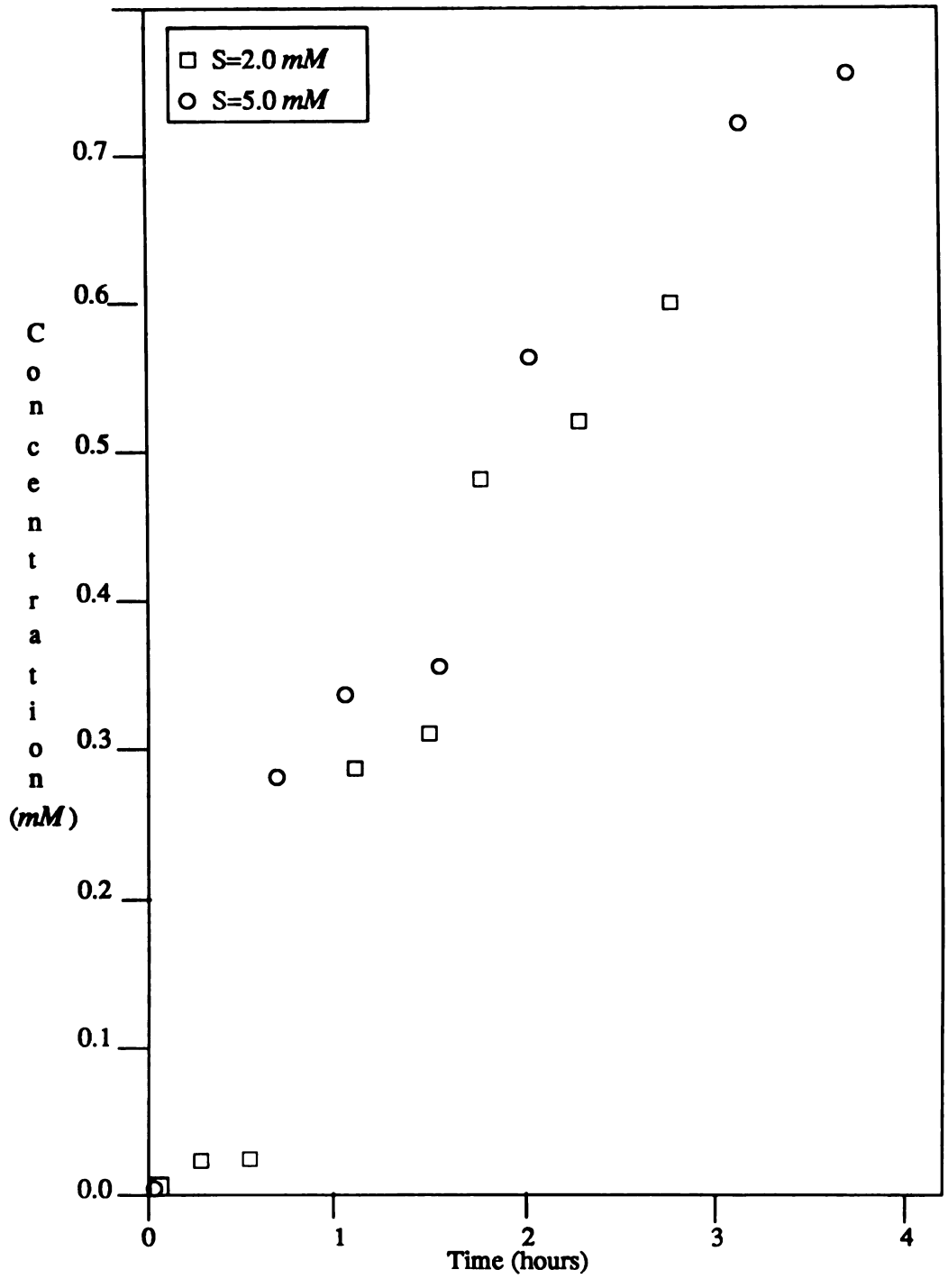

Figure 4.5. Effect of Glutamate Concentration on the Formation of Ammonia for the Backflush Recycle Reactor

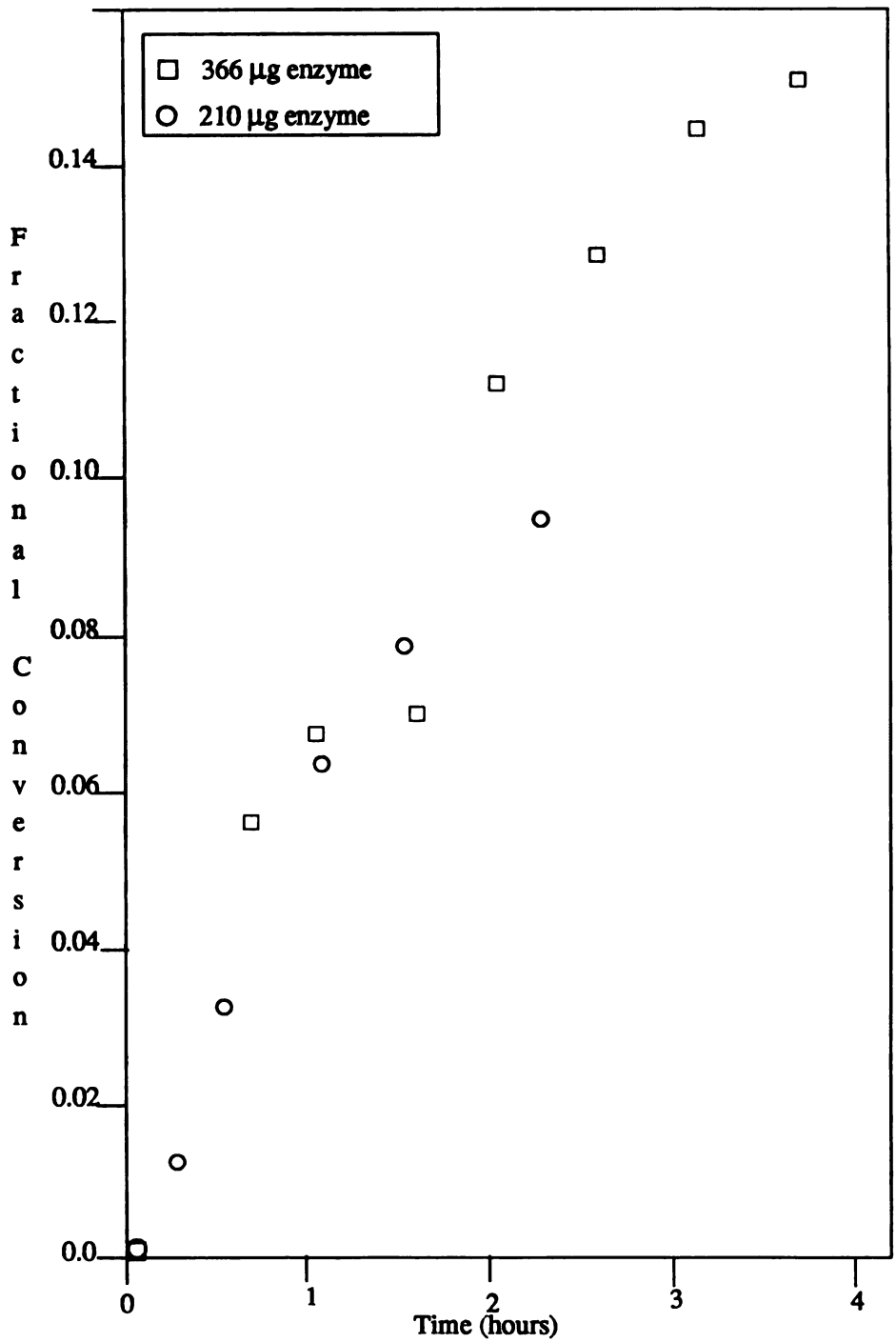

Figure 4.6. Effect of Enzyme Loading on the Fractional Conversion of 5 *mM* Glutamate Solution for the Backflush Recycle Reactor

enzyme available for reaction. An asymptote was not observed in these experiments for the two levels of enzyme loading.

This result seems to indicate that an enzyme loading as high as possible is optimum. However, higher enzyme concentrations restrict the flow through the fiber as disussed in Section 4.3. The flow rate is thus limited by the transmembrane pressure drop. In order to maintain a sufficient flow rate, the maximum pressure drop must be reached. For these fibers and enzyme, no more than 350 μg (10 units) of glutamate oxidase should be immobilized on the fiber to maintain a flow rate of 0.3 ml/min and a pressure drop of less than 10 psi. A larger amount of enzyme on the fiber would lead to either too low a flow rate or too high a transmembrane pressure drop. In addition, an enzyme loading which is too high can waste enzyme by using large quantities of enzyme without providing a significant increase in reaction rate [20]. For this reactor, however, the enzyme loading should never reach that condition because the presure drop limits the enzyme loading.

4.5 Response of the Biosensor

The biosensor was tested for its response to step changes in glutamate concentration. A clean reactor was loaded with 10 units of glutamate oxidase and was backflushed with fresh 2.0 *mM* glutamate solution. The effluent was collected after one pass through the reactor and immediately measured for ammonia. After a period of two hours, the inlet solution was changed to 5.0 *mM* glutamate solution, although a greater step change would have yielded more conclusive results. The effluent was again collected after one pass and assayed for ammonia. The response of the sensor is shown in Figure 4.7. The results were disappointing because the biosensor did not react to the change in glutamate concentration. In fact, the measured concentration actually decreased. After two hours, the biosensor had not responded to the increase in glutamate concentration. The biosensor was backflushed with KPB and tested two more times, but the results were the same.

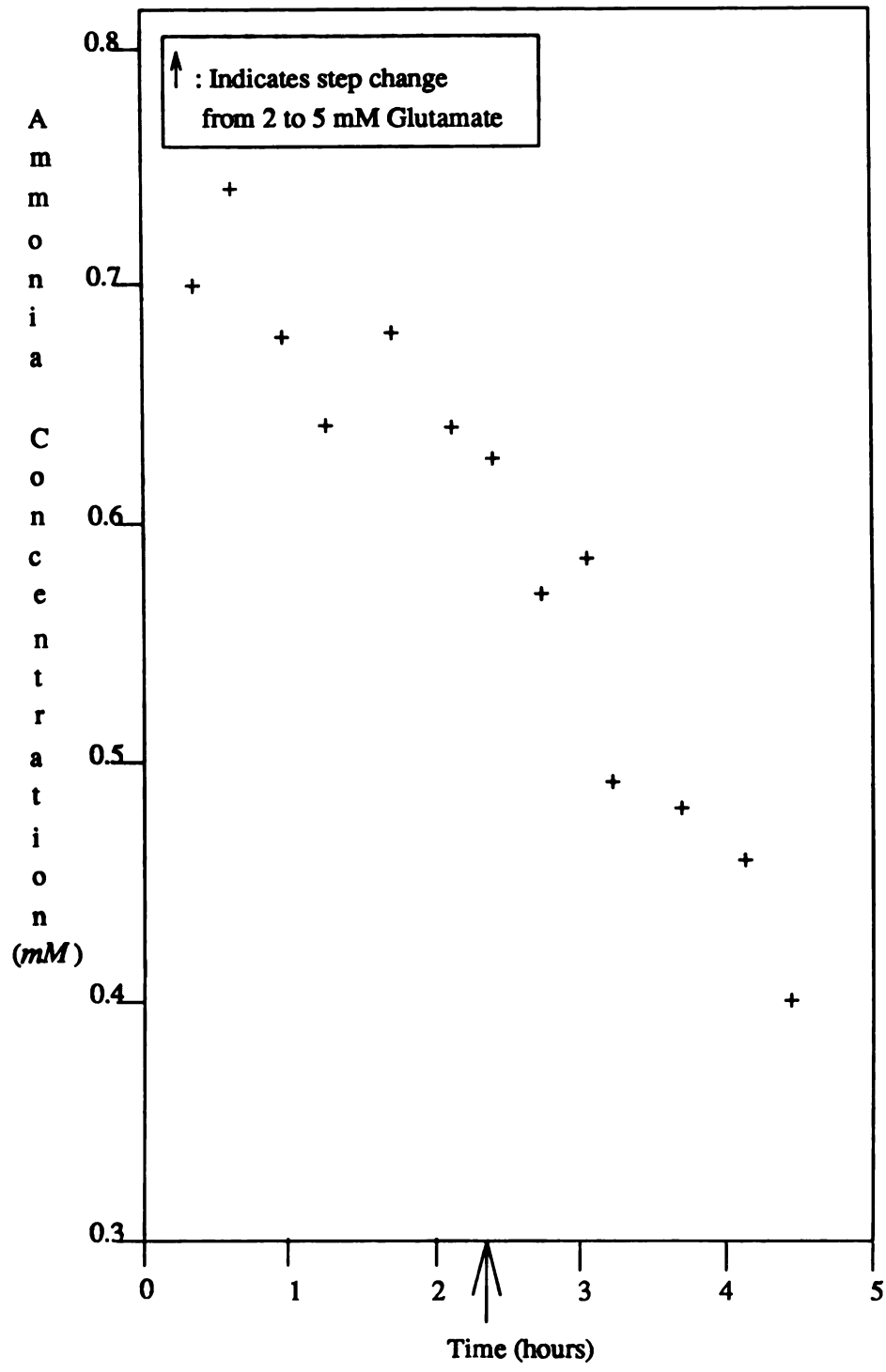

Figure 4.7. Response of Biosensor to Glutamate Concentration

It is apparent that the design of the biosensor system had some deficiencies. Based on the results from Figure 4.5, the expected concentration of one pass through the reactor is 0.03 *mM*. This indicates that a steady state was not reached for the one-pass experiment. The reasons for the poor response of the biosensor are discussed in Section 4.6.

4.6 Intrinsic Immobilized Kinetics

Immobilization can affect the kinetic constants of an enzyme [20]. The intrinsic kinetics were measured for immobilized glutamate oxidase. A reactor loaded with 10 units of glutamate oxidase was run in the recycle mode of operation for 55 hours. The initial glutamate concentration was 5 *mM*.

At regular intervals during the experiment, 1.5 ml samples of the glutamate solution were taken. The samples were analyzed for ammonia concentration with the ammonia electrode.

The results from this experiment were plotted and analyzed using a regression formula of the form $t = f(glutamate\ \ concentration)$, where t represents time and f is some function which fits the data. This equation was differentiated with respect to glutamate concentration, and the reciprocal was taken to obtain the experimental reaction rate, $\frac{d[glu]}{dt} = f([glu])$. The differentiated equation was used in a computer program, described in Appendix B, which estimates the parameters K_m and k. The program uses an iterative scheme which adjusts the two parameters until the theoretical calculations most closely approximate the data. For each data point, the effectiveness factor and the reaction rate were calculated by the Moo-Young and Kobayashi approximation [19] . The effectiveness factor uses the Michaelis-Menten rate expression and is calculated from the K_m, k, enzyme loading, substrate concentration, reactor geometry, and substrate diffusivity [1]. The experimental rate of reaction was calculated by the differentiated

[1] For more details, refer to Equations 27 and 29 in reference [19].

regression formula given above. This program was successfully used by Knob and by Reiken to estimate the kinetic parameters for their immobilized enzymes [20,22,33]. For this reactor-enzyme system, the K_m increased to 2000 mM, and k decreased to 7×10^{-5} $mM\ min^{-1}\ unit^{-1}$ as shown in Table 4.1. As discussed in Section 4.1, the K_m is a measure of the affinity of the enzyme for its substrate. In this case, the K_m increased four orders of magnitude, so the affinity of glutamate oxidase for glutamate decreased significantly. In addition, the k value, which is the intrinsic rate constant, decreased four orders of magnitude. When these two factors are considered together, it is apparent that the reaction rate for this reactor was very slow.

		K_m (mM)	$k\left[\frac{\text{mM}}{min \cdot unit}\right]$
Literature (1, 2, 3, 26)		0.21	—
Experimental	Free Solution	0.24	0.14
	Immobilized	2000	7×10^{-5}

Table 4.1. Kinetic Constants for Glutamate Oxidase

These results may explain the the behavior of the biosensor. A possible consideration is loss of ammonia. The solution was buffered at pH 7.4, so very little ammonia would be lost to the surroundings because the ammonia was in the form of ammonium ion.

An important factor for the poor response of the sensor is the "dead" time of the reactor system. The "dead" time is the amount of time the solution spends in the non-reactive portion of the biosensor system. This includes the time spent in the tubing, the

pump, the shell of the reactor, and the lumen of the fiber. The times that the fluid spent in each part of the system were estimated and are given in Table 4.2. The "dead" time accounts for over 90% of the total time that the solution spends in the biosensor system. This could lead to extensive dispersion effects.

Location	Residence Time
Lumen	1 *min* (a)
Tubing from reservoir to reactor	25 *min* (b)
Tubing from reactor to collection	5 *min* (b)
Shell of reactor	25 *min* (b)
Spongy region (reaction region)	4 *min* (a)
Total	60 *min*
"Dead Time"	56 *min*

(a): calculated
(b): measured

Table 4.2. Residence Times for Each Region of the Reactor

The most likely reason, however, for the poor response is the extremely slow reaction rate that results when glutamate oxidase is immobilized on PM10 fibers. The glutamate oxidase is severely affected by immobilization on the PM10 fibers. This was not apparent from the preliminary experiments. As reported in Section 4.2, the recovered enzyme had an acceptable activity, so the damage to the enzyme is somewhat reversible.

The decreasing ammonia concentration that is evident in Figure 4.7 can also be explained. The reactors were used more than once. Between operations, the reactor were stored without rinsing out the previous glutamate solution since storage of HFERs with its substrate prolongs the life of the reactor [20]. While the reactor was refrigerated in storage, the glutamate oxidase converted glutamate to its products including ammonia. Even though the reactors were backflushed with KPB prior to use, the wash-out of this trapped ammonia can be seen in the decreasing ammonia concentration. If the ammonium ion were adsorbing to the fiber, this would also lead to a decreasing ammonia concentration.

To determine what is actually happening in the fiber, the extent of reaction must be verified independently. This will determine if the reaction is actually proceeding. The immobilized enzyme should also be tested for inhibition by products, since this could also lead to a very slow reaction rate. A residence time distribution should be performed. This will indicate whether channeling is occurring.

Several modifications need to be made to the biosensor. First, the glass shell of the biosensor must be made smaller. Ideally, the inside diameter of the glass shell should be only slightly larger than the outside diameter of the hollow fiber. The tubing should also be changed to a smaller diameter, and the length of tubing should be reduced to a minimum. These two modifications should reduce the "dead" time significantly. The hollow fiber could also be changed to a fiber with a smaller diameter, and a small cartridge could be used. These changes would decrease the "dead" time, but would also significantly change the pressure drop characteristics. If different fibers were used, the loading characteristics and immobilized enzyme kinetics would also change. These changes may improve the response of the biosensor. It may also be possible to shorten the length of the reactor. This should decrease the "dead" time and may improve the response; however, care should be taken that the fiber is long enough to provide a reasonable sample size and to retain a sufficient amount of enzyme. If there is not enough

enzyme, the reaction will be too slow. It may be possible to increase the flow rate through the system. This would lead to a larger transmembrane pressure drop. In this case, the fiber would have to be tested to ensure that it would not suffer adverse effects due to the higher pressure drop. The higher pressure may also have an effect on the glutamate oxidase. The enzyme would need to be tested also to determine the effect of pressure on its activity. In order to overcome the low reaction rate, two changes may be made. Using another fiber may improve the immobilized intrinsic rate constants. Reiken found that PM10 fibers deactivated L-lysine-α-oxidase and used PA10 fibers [20]. Implementation of some or all of these suggested changes should improve the response of this biosensor. The feasibility of this biosensor should be determined in future work.

Chapter 5

Conclusions and Recommendations

This chapter describes the conclusions resulting from the research reported in this thesis. In addition, some implications of this work and how it may affect the development of an enzyme-based biosensor are suggested. Finally, directions for future research work are discussed.

5.1 Thesis Contribution and Recommendations

This thesis has presented the preliminary results of the development of an enzyme-based biosensor. The biosensor consists of glutamate oxidase immobilized in a hollow fiber and the hollow fiber encased in a glass shell. Glutamate, the analyte, was backflushed through the fiber. The enzyme was characterized both in free solution and when immobilized. Different types of hollow fibers were compared, and the best option was chosen. The effects of glutamate concentration and enzyme loading on the sensor were determined, and the response of the biosensor was measured. Recommendations for improving the biosensor were given.

Glutamate oxidase was characterized as an enzyme in free solution and in immobilized form. The free solution intrinsic kinetic constants were measured. The K_m was 0.24 mM, and the k was 0.14 $mM\ unit^{-1}\ min^{-1}$. The K_m compares well with the value found in literature; however, no literature values were found for k. When the glutamate

oxidase was immobilized, the activity of the enzyme was altered. Immobilized glutamate oxidase was ultrafiltered from the fiber, and the kinetic constants were measured. The K_m decreased to 0.07 mM, and the k decreased to 0.08 $mM\ unit^{-1}\ min^{-1}$. This indicates that the affinity of glutamate oxidase for glutamate increased, but that the rate of reaction decreased. The *in situ* immobilized kinetic constants were also measured. In this case, the K_m increased to 2000 mM and k decreased to $7 \times 10^{-5}\ mM\ unit^{-1}\ min^{-1}$. This indicates that the affinity for glutamate decreased when glutamate oxidase was immobilized on PM10 fibers. These values for K_m and k lead to a very slow reaction rate.

Several different hollow fibers were tested for suitability in the biosensor. The PM10 fibers were chosen because they had the highest retention of glutamate oxidase. They retained 80% of the enzyme that was backflush loaded onto the fiber. When the fibers were cleaned and reused, the retention approached 100%, and there was very little loss of enzyme when the fiber was used.

The sensor was evaluated for its pressure drop characteristics. The pressure drop was measured for various flow rates. From these data the resistances of the fiber and of the enzyme were calculated. The resistance of a fiber with enzyme averaged 2.7 times the resistance of a clean fiber. The resistance of fibers with enzyme increased as the amount of enzyme increased. The total resistance of the sensor was divided into a fiber resistance and an enzyme resistance, and their respective permeabilities were calculated. The pressure drop over the fibers was limited to 10 psi which gave a maximum flow rate 0.3ml/min for an "average" fiber.

The effects of certain parameters on the biosensor were measured. The response of the sensor to different glutamate concentrations was measured. As expected, the reaction was faster for the higher concentration of glutamate. When the enzyme loading was lowered, the reaction was slower because there was less enzyme available for reaction.

5.2 Future Work

The results obtained for this thesis appear promising. However, when the biosensor was tested for its response to step changes in glutamate concentration, the biosensor did not respond. This is most likely due to errors in analytical techniques, to the extremely slow reaction rate and to the design of the biosensor. The extent of reaction should be verified with an independent technique, and the enzyme should be tested for inhibition. A residence time distribution should be performed for the backflush flow to determine if channeling is occurring. The "dead" time in the biosensor system is a cause for the poor response, so some modifications need to be made to the biosensor to see if the dead time can be reduced. First, the glass shell needs to be made smaller to reduce the time the analyte spends in the shell. The tubing volume also needs to be reduced. This would decrease the time the solution spends in the tubing. These modifications would change the pressure drop characteristics of the system, so new hydraulic measurements would need to be done. New, smaller fibers may be tested to see if the biosensor can be made smaller. This would also decrease the time the fluid is in the biosensor. It may also be possible to increase the flow rate by increasing the pressure. However, the effect of pressure on the fiber and enzyme would need to be determined. By using other fibers or other enzymes, the reaction rate may be increased. With these modifications, this biosensor has a good chance of becoming a reliable, highly specific on-line biosensor.

Bibliography

[1] Kusakabe, H., Midorikawa, M., Fujishima, T., Kuninaka, A., Yoshino, H., "Purification and Properties of a New Enzyme, from Streptomyces sp. X-119-6 Grown on Wheat Bran", *Agric. Biol. Chem.*, **47** (6), 1323 (1983).

[2] Kusakabe, H., Midorikawa, M., Fujishima, T.,"Rapid and Simple Assay of Glutaminase and Leucine Aminopeptidase Activities of Shoyu Koji Using L-Glutamate Oxidase", *Agric. Biol. Chem.*, **48** (5), 1357 (1983).

[3] Kusakabe, H., Midorikawa, M., Fujishima, T., "Methods for Determining L-Glutamate in Soy Sauce with L-Glutamate Oxidase", *Agric. Biol. Chem.*, **48** (1), 181 (1984).

[4] Zubay, G., *Biochemistry*, Addison-Wesley, Reading, MA (1983).

[5] Guilbault, G., Shu, F., "Enzyme Electrodes Based on the Use of a Carbon Dioxide Sensor. Urea and L-Tyrosine Electrodes", *Anal. Chem.*, **44** (13), 2161 (1972).

[6] White, W., Guilbault, G., "Lysine Specific Enzyme Electrode for Determination of Lysine in Grains and Foodstuffs", *Anal. Chem.*, **50** (11), 1481 (1978).

[7] Belghith, H., Romette, J., Thomas, D., "An Enzyme Electrode for On-Line Determination of Ethanol and Methanol", *Biotech. Bioeng.*, **30**, 1001 (1987).

[8] Romette, J., Cooney, C., " On-Line Mammalian Cell Culture Process Control", *Anal. Letters,* **20** (7), 1069 (1987).

[9] Yamauchi, H., Kusakabe, H., Midorikawa, M., Fujishima, T., Kuninaka, A.,"Enzyme Electrode for Specific Determination of L-Glutamate", *Eur. Congr. Biotechnol.,* 3rd, **1**, 705 (1984).

[10] Aizawa, M., Ikariyama, Y., Kuno, H., "Photovoltaic Determination of Hydrogen Peroxide with a Biophotodiode", *Anal. Letters,* **17** (B7), 555 (1984).

[11] Kim, J., Lee, Y., "Fast Response Glucose Microprobe", *Biotech. Bioeng.,* **31**, 755 (1988).

[12] Murakami, T., Nakamoto, S., Kimura, J., Kuriyama, T., Karube, I., "A Micro Planar Amperometric Glucose Sensor Using an ISFET as a Reference Electrode", *Anal. Letters,* **19** (19&20), 1973 (1986).

[13] Kolisis, F., Thomas, D., "Continuous Assay of Neuraminidase Activity by a Bienzyme System Immobilized in an Artificial Membrane", *Biotech. Bioeng.,* **30**, 160 (1987).

[14] Waterland, L., Michaels, A., Robertson, C., "A Theoretical Model for Enzymatic Cataylsis Using Asymmetric Hollow Fiber Membranes", *AIChE Journal,* **20** (1), 50 (1974).

[15] Waterland, L., Robertson, C., Michaels, A., "Enzymatic Catalysis Using Asymmetric Hollow Fiber Membranes", *Chem. Eng. Commun.,* **2**, 37 (1975).

[16] Tharakan, J., Chau, P., "Operation and Pressure Distribution of Immobilized Cell Hollow Fiber Bioreactors", *Biotech. Bioeng.*, **28**, 1064 (1986).

[17] Davis, M., Watson, L., "Analysis of a Diffusion-Limited Hollow Fiber Reactor for the Measurement of Effective Substrate Diffusivities", *Biotech. Bioeng.*, **27**, 182 (1985).

[18] Webster, I., Shuler, M., "Mathematical Models for Hollow-Fiber Enzyme Reactors", *Biotech. Bioeng.*, **20**, 1541 (1978).

[19] Moo-Young, M., Kobayashi, T., "Effectiveness Factors for Immobilized-Enzyme Reactions", *Can. J. Chem. Eng.*, **50**, 162 (1972).

[20] Reiken, S., "Evaluation of the Co-Immobilization of L-Lysine-α-Oxidase and Catalase in a Hollow Fiber Reactor System", *M.S. Thesis*, Michigan State University (1988).

[21] Jones, C., Yang, R., White, E., "A Novel Hollow-Fiber Reactor with Reversible Immobilization of Lactase", *AIChE Journal*, **34** (2), 293 (1988).

[22] Reiken, S., Knob, R., Briedis, D., "Evaluation of Intrinsic Immobilized Kinetics in Hollow Fiber Reactor Systems", *Enzyme Microb. Technol.*, **12**, 736 (1990).

[23] Lowry, O., Rosebrough, N.J., Farr, A.L., Randall, R.J., "Protein Measurement with the Folin Phenol Reagent", *J. Biol. Chem.*, **193**, 265 (1951).

[24] Hawkins, B., Honigs, D., "A Comparison of Spectroscopic Techniques for Protein Quantification in Aqueous Solutions", *Am. Biotechnol. Lab.*, **5**(6), 26 (1987).

[25] Nakatani, Y., Fujioka, M., Higashino, K., "Enzymic Determination of L-Lysine in Biological Materials", *Anal. Biochem.*, **49**, 225 (1972).

[26] Fujioka, M., Nakatani, Y., "A Kinetic Study of Saccharopine Dehydrogenase Reaction", *Eur. J. Biochem.*, **16**, 180 (1970).

[27] Soda, K., "A Spectrophotometric Microdetermination of Keto Acids with 3-Methyl-2-benzothiazolone Hydrazone", *Agr. Biol. Chem.*, **31** (9), 1054 (1967).

[28] Soda, K., "Microdetermination of D-Amino Acids and D-Amino Acid Oxidase Activity with 3-Methyl-2-benzothiazolone Hydrazone Hydrochloride", *Anal. Biochem.*, **25**, 228 (1968).

[29] Paz, M., Blumenfeld, O., Rojkind, M., Henson, E., Firfine, C., Gallop, P., "Determination of Carbonyl Compounds with N-Methyl Benzothiazolone Hydrazone", *Arch. Biochem. Biophys.*, **109**, 548 (1965).

[30] Sawicki, E., Hauser, T., Stanley, T., Elbert, W., "The 3-Methyl-2-benzothiazolone Hydrazone Test", *Anal. Chem.*, **33** (1), 93 (1961).

[31] Wilkinson, G., "Statistical Estimations in Enzyme Kinetics", *Biochem. J.*, **80**, 324 (1961).

[32] Belter, P., Cussler, E., Hu, W., *Bioseparations: Downstream Processing for Biotechnology*, John Wiley & Sons, New York (1988).

[33] Knob, R., "Performance of β-Galactosidase from *Bacillus stearothermophilus* in Hollow Fiber Reactors", *M.S. Thesis*, Michigan State University (1988).

Appendix A

This appendix describes the program that implements the Wilkinson method to statistically determine the K_m and v_{max} using Michaelis-Menten kinetics.

The program was written in the FORTRAN language. The program contains three basic components. The first component of the main program reads the input file name, and opens the corresponding file to input the data. For each input file, the program creates a corresponding output file by replacing the original extension of the input file name with a "out" extension. The second component of the main program performs the Wilkinson's method. Finally, the third component of the program calculates the standard error for K_m and v_{max}.

The description of the source code of the program follows.

```
C*********************************************************************
C  This program uses the Wilkinson method to statistically determine the
C  the Km and vmax using Michaelis-Menton kinetics.
C*********************************************************************

      PROGRAM WILK
      PARAMETER(J=6)
      CHARACTER*32  INFILE,OUTFIL,GFILE(J),GFSTAT,FNAME
      INTEGER N,I
      REAL*8 S(50),V(50),KM,VMAX,X(50),Y(50),ALPHA,BETA,GAMMA,DELTA
      REAL*8 ALPHA2,GAMMA2,BETA2,DELTA2,EPS2,SUMV2,F(50),F2(50),DEL2,B1
      REAL*8 B2,SD2,SD,VM,K,SDVM,SDK,EPSILON,DEL
C
C     Read data input file name,
C
      CALL FILSET(INFILE,OUTFIL,GFILE)
C
      OPEN(60,FILE=INFILE,STATUS='OLD')
      OPEN(61,FILE=OUTFIL,STATUS='UNKNOWN')
C
C     Read the data
C
       READ(60,*) N
      DO 10  I=1,N
       READ(60,*) S(I),V(I)
 10  CONTINUE
C
C     Perform the Wilkinson's method
C
      ALPHA=0.0
      BETA=0.0
      GAMMA=0.0
      DELTA=0.0
      EPSILON=0.0

      DO 20 I=1,N
        V3=V(I)**3
        V4=V(I)**4
        ALPHA=ALPHA + V3
        BETA=BETA + V4
        GAMMA=GAMMA + V3/S(I)
        DELTA=DELTA + V4/S(I)
        EPSILON=EPSILON + V4/S(I)**2
 20  CONTINUE
```

```
      DEL=ALPHA*EPSILON - GAMMA*DELTA

      KM=(BETA*GAMMA - ALPHA*DELTA)/DEL
      VMAX=(BETA*EPSILON - DELTA**2)/DEL

      WRITE(61,*)'Km = ',KM,'Vmax = ',VMAX

C
C     This section calculates the standard error for Km and vmax
C

      ALPHA2=0.0
      GAMMA2=0.0
      BETA2=0.0
      DELTA2=0.0
      EPS2=0.0
      SUMV2=0.0

      DO 30 I=1,N
       F(I)=VMAX*S(I)/(S(I)+KM)
       F2(I)=-F(I)/(S(I)+KM)
       ALPHA2=ALPHA2+F(I)**2
       GAMMA2=GAMMA2+F(I)*F2(I)
       BETA2=BETA2+F2(I)**2
       DELTA2=DELTA2+V(I)*F(I)
       EPS2=EPS2+V(I)*F2(I)
       SUMV2=SUMV2+V(I)**2
   30  CONTINUE

      DEL2=ALPHA2*BETA2-GAMMA2**2
      B1=(BETA2*DELTA2-GAMMA2*EPS2)/DEL2
      B2=(ALPHA2*EPS2-GAMMA2*DELTA2)/DEL2
      SD2=(SUMV2-B1*DELTA2-B2*EPS2)/(N-2)
      SD=SQRT(SD2)


      VM=B1*VMAX
      K=KM+B2*B1
      SDVM=VMAX*SD*(BETA2/DEL2)**0.5
      SDK=(SD/B1)*SQRT(ALPHA2/DEL2)


      WRITE(61,*)'Km(TRUE) = ',K,'Vmax(TRUE) = ',VM
      WRITE(61,*)'SD(Km) = ',SDK,'SD(Vmax) = ',SDVM

      STOP
```

```
      END

C*********************************************************************
C     Routine to read data input file, and set up the output files,
C*********************************************************************
      SUBROUTINE FILSET(INFILE,OUTFIL,GFILE)

      PARAMETER(J=6)
      INTEGER DONE
      CHARACTER*32  INFILE,OUTFIL,FNAME


      DO 120 I = 1,32
       INFILE(I:I) = ' '
       OUTFIL(I:I) = ' '
  120 CONTINUE

       WRITE(*,1000)
       READ(*,'(A)') INFILE

      DONE=0
      I=1
      DO WHILE ((I.LE.32).AND.(DONE.EQ.0))
       IF (INFILE(I:I).EQ.'.') THEN
C
C     If the input file name includes an extension, use name as is,
C
         FNAME = INFILE(1:I-1)
         DONE=1
       ELSEIF (INFILE(I:I).EQ.' ')THEN
C
C     Else add the extension "dat" to the name of the file.
C
         FNAME = INFILE(1:I-1)
         INFILE(I:I+3) = '.dat'
         DONE=1
       ENDIF
       I=I+1
      END DO
      LFN = I-1
      LP1 = LFN+1
      LP4 = LFN+7

      OUTFIL = FNAME
      OUTFIL(LP1:LP4) = '.out'
```

```
1000 FORMAT(' ',//,2X,'PROGRAM EXECUTION BEGINS...',//,2X,
  + 'INPUT DATA FILE NAME, [DEFAULT EXTENSION =.dat]:',/)


   RETURN
   END
```

Appendix B

This appendix describes the program used to estimate the parameters K_m and k. The program uses an iterative scheme which adjusts the two parameters until the theoretical calculations most closely approximate the data. For each data point, the effectiveness factor and the reaction rate were calculated by the Moo-Young and Kobayashi approximation. The effectiveness factor uses the Michaelis-Menten rate expression and is calculated from the K_m, k, enzyme loading, substrate concentration, reactor geometry, and substrate diffusivity.

The program is written in the FORTRAN language. In the first part of the main program, the initial conditions and initial search parameters are set and the procedure pattern is called with the required parameters. The subroutine patern invokes the subroutine calcs through subroutine proc to determine the Thiele modulus for the enzyme reaction from the kinetic and diffusion parameters, and to evaluate the effectiveness factor based on Moo-Young and Kobayashi approximation method.

The description of the source code of the program follows.

```
C*****************************************************************
C     The patern search routine is invoked by calling the procedure patern.
C     It also contains the initial values of the parameters and other
C     formatting instructions for patern.
C     The data to be fit by a transfer function are the
C     input (U) and the process output (X) values.
C*****************************************************************

      DIMENSION P(1000), STEP(1000)
C
C     Set initial conditions and initial search parameters
C
      P(1) = .070
      P(2) = 2.184
      STEP(1) = .1
      STEP(2) = 1.
      IO = 2
      NP = 3
      NRD = 3
C
C     Call the procedure pattern with the required parameters.
C
      CALL PATERN(NP,P,STEP,NRD,IO,COST)
      STOP
      END

C*****************************************************************
C     The purpose of the following subroutines is to achieve
C     compatibility with the optimization subroutine patern.
C     They simulate a process using discrete difference
C     equations and compare the simulation output with
C     the actual output (read in through a data file),
C     calculating an error or "cost" associated with that
C     simulation.  The procedure patern uses these subroutines
C     iteratively in order to find the optimum set of transfer
C     function parameters to fit the data.
C*****************************************************************

      SUBROUTINE PROC(P,COST)
      DIMENSION P(1000), STEP(1000)
C
C     Initialize arrays and define parameters
C
      COST=0.0
C
```

```
C     Perform simulation and calculate error
C
      CALL CALCS(P,COST)
      RETURN
      END
C
C
C
      SUBROUTINE BOUNDS (P,IOUT)
      DIMENSION P(1000), STEP(1000)
      IOUT = 0
      IF (P(1) .LT. 0.) IOUT = 1
      IF (P(2) .LT. 0.) IOUT = 1
      RETURN
      END

     SUBROUTINE PATERN(NP,P,STEP,NRD,IO,COST)

C-----THE SIZE OF B1,B2,T,AND S NEED ONLY BE EQUAL TO THE NUMBER OF PAR

     DIMENSION P(1000),STEP(1000),B1(100),B2(100),T(100),S(100)

C*************************************************************
C     The following command allows patern to use an integer
C     variable as the third parameter P(3).
C*************************************************************

C
C     Starting point
C
     L=1
     ICK=2
     ITTER=0
     DO5 I=1,NP
     B1(I)=P(I)
     B2(I)=P(I)
     T(I)=P(I)
  5  S(I)=STEP(I)*10.
C
C    Initial boundary check and cost evaluation
C
     CALL BOUNDS(P,IOUT)
     IF(IOUT.LE.0)GOTO10
           IF(IO.LE.0)GOTO6
           WRITE(05,1005)
           WRITE(05,1000)(J,P(J),J=1,NP)
```

```
 6  RETURN
 10  CALL PROC(P,C1)
           IF(IO.LE.0)GOTO11
           WRITE(05,1001)ITTER,C1
           WRITE(05,1000)(J,P(J),J=1,NP)
C
C     Beginning of pattern search strategy
C
 11  DO99 INRD=1,NRD
     DO12 I=1,NP
 12  S(I)=S(I)/10.

           IF(IO.LE.0)GOTO20
           WRITE(05,1003)
           WRITE(05,1000)(J,S(J),J=1,NP)
 20  IFAIL=0.0
C
C    PRETURBATION ABOUT T
C

     DO30 I=1,NP
     IC=0
 21  P(I)=T(I)+S(I)
     IC=IC+1
     CALL BOUNDS(P,IOUT)
     IF(IOUT.GT.0)GOTO23
     CALL PROC(P,C2)
           L=L+1
           IF(IO.LT.3)GOTO22
           WRITE(05,1002)L,C2
           WRITE(05,1000)(J,P(J),J=1,NP)
 22  IF(C1-C2)23,23,25
 23  IF(IC.GE.2)GOTO24
     S(I)=-S(I)
     GOTO21
 24  IFAIL=IFAIL+1
     P(I)=T(I)
     GOTO30
 25  T(I)=P(I)
     C1=C2
 30  CONTINUE
     IF(IFAIL.LT.NP)GOTO35
     IF(ICK.EQ.2)GOTO90
     IF(ICK.EQ.1)GOTO35
     CALL PROC(T,C2)
           L=L+1
```

```
          IF(IO.LT.2)GOTO31
          WRITE(05,1002)L,C2
          WRITE(05,1000)(J,T(J),J=1,NP)
31  IF(C1-C2)32,34,34
32  ICK=1
    DO33 I=1,NP
    B1(I)=B2(I)
    P(I)=B2(I)
33  T(I)=B2(I)
    GOTO20
34  C1=C2
35  IB1=0
    DO39 I=1,NP
    B2(I)=T(I)
    IF(ABS(B1(I)-B2(I)).LT.1.0E-20)IB1=IB1+1
39  CONTINUE
    IF(IB1.EQ.NP)GOTO90
    ICK=0
          ITTER=ITTER+1
          IF(IO.LT.2)GOTO40
          WRITE(05,1001)ITTER,C1
          WRITE(05,1000)(J,T(J),J=1,NP)
C
C   Acceleration step
C
40  SJ=1.0
    DO45 II=1,11
    DO42 I=1,NP
    T(I)=B2(I)+SJ*(B2(I)-B1(I))
42  P(I)=T(I)
    SJ=SJ-.1
    CALL BOUNDS(T,IOUT)
    IF(IOUT.LT.1)GOTO46
    IF(II.EQ.11)ICK=1
45  CONTINUE
46  DO47 I=1,NP
47  B1(I)=B2(I)
    GOTO20
90  DO91 I=1,NP
91  T(I)=B2(I)
99  CONTINUE
    DO100 I=1,NP
100 P(I)=T(I)
    COST=C1
          IF(IO.LE.0)RETURN
          WRITE(05,1004)L,C1
```

```
          WRITE(05,1000)(J,P(J),J=1,NP)
      RETURN
1000  FORMAT(3(35X,I7,5X,E13.6/))
1001  FORMAT(//1X13HITERATION NO. ,I5/5X,5HCOST= ,E15.6,20X,
     1  10HPARAMETERS)
1002  FORMAT(10X3HNO.,I4, 8X5HCOST=,E15.6)
1003  FORMAT(/1X28HSTEP SIZE FOR EACH PARAMETER  )
1004  FORMAT(1H113HANSWERS AFTER ,I3,2X,23HFUNCTIONAL EVALUATIONS  //
     1  5X5HCOST=,E15.6,20X,18HOPTIMAL PARAMETERS  )
1005  FORMAT(1H135HINITIAL PARAMETERS OUT OF BOUNDS       )
      END

      SUBROUTINE CALCS(P,COST)
C*************************************************************************
C     Determine enzyme reaction Thiele modulus from
C     kinetic and diffusion parameters and determine effectiveness
C     factor from Moo-Young and Kobayashi approximation.
C     Use of this Model to predict reaction rate for various
C     micromoles of lysine reacted.
C*************************************************************************
      Dimension Q(20),P(100)
      open (60,file='intrnsc.dat.',status='old')
C
C     Initialize values
C
       EKM=P(1)
       DS = 6.5 E-7
       EK=P(2)
       VOL = 0.469
       VOL1 = 100.
      SA = 7.7132
       COST=0.0
C
C     Read data and calculate modulus and effectiveness
C
      Do 50 J=1, 11
      E0= 0.3660
      Read (60,*) S
C
C     Calculate effectiveness factor
C
            VM = EK * E0
            VP = EK * S / (S + EKM)
C
C     Calculate thiele modulus
C
```

```
            EL = VOL/ SA
            H = EL * SQRT(VM / (120.0*DS*S))
            B1 = EKM / S
            B2 = 1.0
            EI2 = 1.0 / (B2**2) * (B2 - (B1*LOG((B1+B2)/B1)))
            DV = SQRT(EI2)
            TM = (H / (B1+B2)) * (1.0/ DV)
      Eff=(1.0/tm+B1*tanh(tm)/tm)/(1.0+B1)
      R=(eff*VP*E0)
      Rexp= (1.0/60.0)/(-6.579 + 10.728*S - 9.342*S**2 + 1.4872*S**3)
      Cost =cost+abs((R-Rexp)**2)
       VOL1 = VOL1 - 1.5
50    CONTINUE
      close (60)
      RETURN
      END
```